



Revista Mexicana de Ciencias
Geológicas

ISSN: 1026-8774

rmcg@geociencias.unam.mx

Universidad Nacional Autónoma de
México
México

González-Becuar, Elizard; Pérez-Segura, Efrén; Vega-Granillo, Ricardo; Solari, Luigi;
González-León, Carlos M.; Solé, Jesús; López Martínez, Margarita
Laramide to Miocene syn-extensional plutonism in the Puerta del Sol area, central
Sonora, Mexico
Revista Mexicana de Ciencias Geológicas, vol. 34, núm. 1, marzo, 2017, pp. 45-61
Universidad Nacional Autónoma de México
Querétaro, México

Available in: <http://www.redalyc.org/articulo.oa?id=57250506005>

- How to cite
- Complete issue
- More information about this article
- Journal's homepage in redalyc.org

redalyc.org

Scientific Information System

Network of Scientific Journals from Latin America, the Caribbean, Spain and Portugal

Non-profit academic project, developed under the open access initiative

Laramide to Miocene syn-extensional plutonism in the Puerta del Sol area, central Sonora, Mexico

Elizard González-Becuar^{1,*}, Efrén Pérez-Segura¹, Ricardo Vega-Granillo¹, Luigi Solari², Carlos M. González-León³, Jesús Solé⁴, and Margarita López Martínez⁵

¹ Departamento de Geología, Universidad de Sonora, Blvd. Encinas y Rosales, 83000, Hermosillo, Sonora, Mexico, Present address, Grupo México, Centro de Investigaciones, Centenario y Turquesa s/n, Colonia La Prieta, 33800, Hidalgo del Parral, Chihuahua, Mexico.

² Universidad Nacional Autónoma de México, Centro de Geociencias, Campus Juriquilla, 76230, Querétaro, Qro., Mexico.

³ Universidad Nacional Autónoma de México, Instituto de Geología, Estación Regional del Noroeste, 83000, Hermosillo, Sonora, Mexico.

⁴ Universidad Nacional Autónoma de México, Instituto de Geología, Ciudad Universitaria, 04510, Cd. de México, Mexico.

⁵ Departamento de Geología, Centro de Investigación Científica y de Educación Superior de Ensenada (CICESE), Carretera Ensenada-Tijuana No. 3918, 22860, Ensenada, Baja California, Mexico.

*elizard.gonzalez@mm.gmx.com

ABSTRACT

Plutonic rocks of the Puerta del Sol area, in central Sonora, represent the extension to the south of the El Jaralito batholith, and are part of the footwall of the Sierra Mazatán metamorphic core complex, whose low-angle detachment fault bounds the outcrops of plutonic rocks to the west. Plutons in the area record the magmatic evolution of the Laramide arc and the Oligo-Miocene syn-extensional plutonism in Sonora. The basement of the area is composed by the ca. 1.68 Ga El Palofierral orthogneiss that is part of the Caborca block. The Laramide plutons include the El Gato diorite (71.29 ± 0.45 Ma, U-Pb), the El Pajarito granite (67.9 ± 0.43 Ma, U-Pb), and the Puerta del Sol granodiorite (49.1 ± 0.46 Ma, U-Pb). The younger El Oquimonis granite (41.78 ± 0.32 Ma, U-Pb) is considered part of the scarce magmatism that in Sonora records a transition to the Sierra Madre Occidental magmatic event. The syn-extensional plutons are the El Garambullo gabbro (19.83 ± 0.18 Ma, U-Pb) and the Las Mayitas granodiorite (19.2 ± 1.2 Ma, K-Ar). A migmatitic event that affected the El Palofierral orthogneiss, El Gato diorite, and El Pajarito granite between ca. 68 and 59 Ma might be related to the emplacement of the El Pajarito granite. The plutons are metaluminous to slightly peraluminous, with the exception of El Oquimonis granite, which is a peraluminous two-mica, garnet-bearing granite. They are mostly high-K calc-alkaline with nearly uniform chondrite-normalized REE and primitive-mantle normalized multielemental patterns that are characteristic of continental margin arcs and resemble patterns reported for other Laramide granites of Sonora. The Laramide and syn-extensional plutons also have Sr, Nd and Pb isotopic ratios that plot within the fields reported for Laramide granites emplaced in the Caborca terrane in northwestern and central Sonora. Nevertheless, and despite their geochemical affinity to continental magmatic arcs, the El Garambullo gabbro and Las Mayitas granodiorite are syn-extensional plutons that were emplaced at ca. 20 Ma during development of the Sierra Mazatán

metamorphic core complex. The $^{40}\text{Ar}/^{39}\text{Ar}$ and K-Ar ages obtained for the El Palofierral orthogneiss, the Puerta del Sol granodiorite, the El Oquimonis granite, and the El Garambullo gabbro range from 26.3 ± 0.6 to 17.4 ± 1.0 Ma and are considered cooling ages associated with the exhumation of the metamorphic core complex.

Key words: Laramide magmatism; syn-extensional plutonism; geochronology; geochemistry; Sr-Nd-Pb isotopes; Sonora; Mexico.

RESUMEN

El área de Puerta del Sol, en el centro de Sonora, se encuentra en la parte sur del batolito El Jaralito y es parte de la placa inferior del complejo de núcleo metamórfico de la Sierra Mazatán, cuya falla de despegue limita sus afloramientos en su parte occidental. La geología la forman varios plutones que registran la evolución magmática del arco Laramide hasta el plutonismo sinextensional del Oligoceno-Mioceno de Sonora. El basamento del área lo forma el ortogneis El Palofierral cuya edad de ca. 1.68 Ga (U-Pb) lo hace pertenecer al basamento del bloque Caborca. Los plutones laramídicos incluyen a la diorita El Gato (71.29 ± 0.45 Ma, U-Pb), el granito El Pajarito (67.9 ± 0.43 Ma, U-Pb) y la granodiorita Puerta del Sol (49.1 ± 0.46 Ma, U-Pb). El granito El Oquimonis (41.78 ± 0.32 Ma, U-Pb) es un plutón más joven considerado parte del escaso magmatismo regional transicional al de la Sierra Madre Occidental. Los plutones sinextensionales están representados por el gabro El Garambullo (19.83 ± 0.18 Ma, U-Pb) y la granodiorita Las Mayitas (19.2 ± 1.2 Ma, K-Ar). Un evento migmatítico que ocurrió entre ca. 68 y 59 Ma afectó al ortogneis El Palofierral, a la diorita El Gato y al granito El Pajarito y pudiera estar relacionado a la intrusión de este último. Los plutones del área son metaluminosos a ligeramente peraluminosos, con excepción del granito El Oquimonis que es peraluminoso, de dos micas y con granate. Estas rocas son principalmente calcialcalinas, altas en K,

con patrones muy similares en diagramas de tierras raras normalizados a condrita y diagramas multielementales normalizados a manto primitivo, los cuales indican firmas características del magmatismo de arco en zonas de subducción asociadas a márgenes continentales. Tienen además relaciones isotópicas de Nd, Sr y Pb similares a valores reportados para los granitos laramídicos emplazados en rocas del terreno Caborca en el noroeste y centro de Sonora. Sin embargo, y a pesar de su afinidad geoquímica con magmatismo de arco, el gabro El Garambullo y la granodiorita Las Mayitas son plutones emplazados durante la extensión asociada al complejo de núcleo metamórfico de la Sierra Mazatán, tal como lo indican sus edades de ca. 20 Ma. Las edades $^{40}\text{Ar}/^{39}\text{Ar}$ y K-Ar obtenidos para el ortogneis El Palofieral, la granodiorita Puerta del Sol, el granito El Oquimonis y el gabro El Garambullo tienen un rango de 26.3 ± 0.6 a 17.4 ± 1.0 Ma y se consideran edades de enfriamiento asociadas a la exhumación del complejo de núcleo metamórfico de la Sierra de Mazatán.

Palabras clave: magmatismo Laramide; plutonismo sinextensional; geocronología; geoquímica; isótopos de Sr-Nd-Pb; Sonora, México.

INTRODUCTION

The geology of the Puerta del Sol area, located in central Sonora, has been poorly reported despite its location at an intermediate position between the well-studied El Jaralito batholith (Roldán-Quintana, 1989, 1991) to the north and the Sierra Mazatán core complex to the south (Figure 1). In this regard, this area records the southern extension of the batholithic magmatism related to the Laramide arc, and

given its position in the footwall of the Sierra de Mazatán core complex (Anderson et al., 1980; Wong and Gans, 2008), it also records the Miocene syn-extensional plutonic evolution.

Late Cretaceous to Eocene volcanic sequences and associated plutons comprise an important fraction of the outcropping rocks of Sonora and are part of the Laramide magmatic arc constrained between 90 and 40 Ma by Damon et al. (1983). Development and eastward migration of the arc in southwestern North America during Late Cretaceous time was postulated to be related to progressive shallowing of the subducting Farallon plate (Coney and Reynolds, 1977; Dickinson and Snyder, 1978; Cuéllar-Cárdenas et al., 2012). Subsequent slab steepening of the Farallon plate that started in Eocene-Oligocene time produced westward regression of magmatism toward the continental-margin (Clark et al., 1982), which was accompanied by upper crustal extension and core complex exhumation related to Basin and Range tectonism (Calmus et al., 2011).

The volcanic succession of the Laramide magmatic arc was assigned to the Tarahumara Formation (Wilson and Rocha, 1949, McDowell et al., 2001), while plutons and batholiths were assigned to the Sonoran batholith (Damon et al., 1983). Outcrops of these rocks are widespread in Sonora, and recent contributions have improved the knowledge of their regional stratigraphy, geochronology, geochemical and radiogenic isotopic composition, to better constrain the timing, nature and implication of basement variations, associated mineralization, and petrogenesis (Roldán-Quintana, 1991, McDowell et al., 2001, Valencia-Moreno et al., 2001, Valencia-Moreno et al., 2003, Iriondo et al., 2004, Barra et al., 2005, Housh and McDowell, 2005, Nourse et al., 2005, Valencia et al., 2005, Nogues-Alcántara et al., 2007, Roldán-Quintana et al., 2009, Pérez-Segura et al., 2009, González-León et al., 2011, Pérez-Segura et al., 2013, Del Río Salas et al., 2013).

In central Sonora, the Laramide magmatism is best represented by the El Jaralito batholith (Roldán-Quintana, 1989, 1991) (Figure 1). Although this batholith was originally studied in sierra Aconchi and in the northern part of sierra El Jaralito (Roldán-Quintana, 1989, 1991; González-León et al., 2011), it extends to the south in a ca. 100 km-long and up to 30 km-wide belt of plutons that end in Sierra Mazatán (Figure 1). Furthermore, the El Jaralito batholith not only holds a nearly complete history of Laramide plutonism but it also records the late Cenozoic magmatic events associated with the extensional phase that exhumed the Sierra Mazatán metamorphic core complex and the batholith itself.

Within El Jaralito batholith, Laramide magmatism is represented by dioritic to granitic plutons, including two-mica peraluminous granites, that range in age from ~70 to ~50 Ma (González-León et al., 2011), whereas in its flanks there are Oligocene-Miocene metamorphic core complexes of Sierra Mazatán, Sierra El Jaralito and Sierra Aconchi (Coney, 1980; Anderson et al., 1980; Nourse et al., 1994; Vega-Granillo

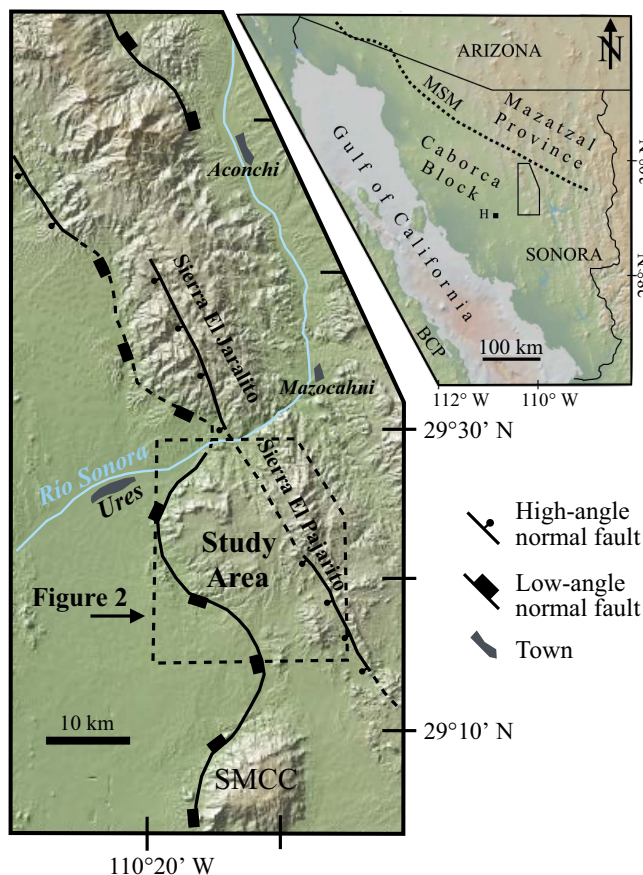


Figure 1. Digital elevation map (taken from GeoMapApp at www.geomapapp.org) indicating the location of physiographic features and localities of central Sonora referred in the text. The location of the studied Puerta del Sol area is indicated by the dashed rectangle in the southern part of the area. The El Jaralito batholith (Roldán-Quintana, 1991) crops out in sierras El Jaralito and Aconchi in the northern part of the map and in this work it is assumed to continue south into sierras El Pajarito and Mazatán. The low angle fault in the western part of the range (taken from Calmus et al., 2011) corresponds to the west-dipping detachment fault associated to metamorphic core complex exhumation in this region, including the Sierra Mazatán metamorphic core complex (SMCC). Inset map of Sonora in the upper right shows the location of the El Jaralito batholith region, the Mazatán and Caborca cratonic blocks. The boundary of these blocks (thick dashed line) is interpreted to be the Mojave-Sonora megashear (MSM).

and Calmus, 2003; Wong and Gans, 2003, 2008; Lugo Zazueta, 2006; Wong *et al.*, 2010, Calmus *et al.*, 2011) (Figure 1).

The El Jaralito batholith intrudes a Proterozoic basement composed of ~1.7 Ga and ~1.1 Ga granites of the Caborca terrane, a Neoproterozoic, Paleozoic and Mesozoic sedimentary succession that reaches an estimated thickness of 12 km, as well as the contemporaneous ~4 km thick volcanic succession of the Tarahumara Formation (González-León *et al.*, 2011).

The purpose of this work is to detail the geology of the Puerta del Sol quadrangle located just south of the El Jaralito batholith, and 15 km to the north of the Sierra Mazatán core complex (Figure 1) (González-Becuar, 2013). The rocks of this area comprise an almost continuous record of plutonism that illustrates the transition from the Laramide magmatic arc event to the Oligo-Miocene core complex extension in central Sonora. Our work is based on field cartography at the 1:50,000 scale, U-Pb, K-Ar and $^{40}\text{Ar}/^{39}\text{Ar}$ geochronology that helps to constrain the age of the magmatic events, while major, trace and Sr-Nd-Pb isotope geochemistry helps to infer the petrogenesis of the different igneous events.

GEOLOGY OF THE STUDY AREA

The Puerta del Sol area is located 70 km E-NE of the city of Hermosillo, within coordinates 110° 00' to 110° 20' W and 29° 15' to 29° 30' N. It covers almost the complete 1:50,000 topographic chart H12D33 edited by INEGI (2004) and includes the El Pajarito and El Batamote sierras in its eastern and southern parts, respectively (Figure 2).

The geology of the area was first reported by Radelli (1986) in a general map where he recognized and named some of the plutons that are herein described in detail. Radelli (1986) named the El Pajarito, El Oquimonis, Garambullo, and Las Mayitas plutons, and his nomenclature is followed in this paper. Anderson *et al.* (1980) named the Puerta del Sol granodiorite and reported a U-Pb age of 57 ± 2 Ma for this pluton. In addition to these plutons, we recognized the El Palofierrall orthogneiss, El Gato diorite and the occurrence of widespread zones of migmatization. Damon *et al.* (1983) reported a zircon U-Pb age of 57 ± 3 Ma (originally reported by Damon and Mauger, 1966) for a “granitic porphyry” sample from the Puerta del Sol pluton.

Anderson *et al.* (1980) suggested that the Puerta del Sol area was part of the lower plate of a metamorphic core complex, which Nourse *et al.* (1994) later referred to as the Puerta del Sol domain. Vega-Granillo and Calmus (2003) considered the Puerta del Sol area as a continuation of the Sierra Mazatán metamorphic core complex shear zone, which was mainly active from ~25 and 16 Ma (Wong and Gans, 2008). The denudation of this core complex was mostly driven along a major detachment fault that crops out in its western part and that we informally refer herein as the Sierra Mazatán detachment fault (Figure 2).

The metamorphic and plutonic units of the study area include the El Palofierrall orthogneiss, which is part of the Proterozoic basement of the region, Laramide plutons and associated migmatite zones, and plutons that were synchronically emplaced with the exhumation of the metamorphic core complex. The Laramide plutons are the El Gato diorite, El Pajarito, Puerta del Sol and El Oquimonis granites and syn-extensional plutons are the El Garambullo gabbro and the Las Mayitas granodiorite. Two regional swarms of dikes that intrude these rocks are briefly described. Restricted outcrops of metasedimentary rocks of probable Paleozoic age also occur as screens or isolated pendants on younger plutons, while in the eastern and western parts of the area there are outcrops of undifferentiated volcanic rocks, which were tentatively assigned to the Tarahumara Formation (Figure 2). The valley located to

the west of the detachment fault is partially occupied by sedimentary and volcanic rocks of Miocene age that represent continental deposits accumulated on the hanging-wall during core-complex formation (Calles-Montijo, 1999; Vega-Granillo and Calmus, 2003; Wong and Gans, 2008).

El Palofierrall orthogneiss

El Palofierrall orthogneiss was originally mapped and referred to as “granite gneiss” by Radelli (1986). This is the oldest unit in the study area, and constitutes small hills along the central part of the area, with the best outcrops found along the El Palofierrall and El Bamuco creeks (Figure 2). The orthogneiss is foliated, leucocratic to mesocratic, and coarse-grained, with K-feldspar porphyroclasts up to 5 cm in size (Figure 3a). The main mineral assemblage is K-feldspar (orthoclase and subordinate microcline), quartz, biotite, plagioclase (An_{20-30}), opaque minerals and muscovite. Feldspar porphyroclasts show micro-boudinage and quartz-filled pressure shadows. Quartz grains are stretched with strong undulose extinction and biotite occurs as euhedral elongate crystals displaying incipient chloritization. Muscovite is a secondary or metamorphic mineral formed after biotite and plagioclase. This rock shows mineral foliation and banding, as well as large-scale folding indicated by regional dip of the foliation. Dilation-structured migmatites (discussed below) consisting of quartz + feldspar + biotite leucosomes are heterogeneously dispersed within this unit.

El Gato diorite

This pluton is exposed in a small area in the central part of the Sierra El Pajarito (Figure 2). The pluton consists of hypidiomorphic, holocrystalline, medium- to coarse-grained mesocratic rocks with plagioclase, orthoclase, quartz, biotite and subordinate hornblende and pyroxene (Figure 3b). Plagioclase (An_{20-40}) is euhedral, commonly glomeroporphyritic and occasionally myrmekitic, whereas orthoclase is anhedral and is affected by moderate sericitization and secondary muscovite development. Quartz crystals are anhedral with undulose extinction, and mostly fill interspaces between feldspars. This pluton is affected by migmatization in the northern part of its outcrop (Figure 2).

Migmatites

A zone of migmatization occurs in the east-central part of the study area (Figure 2), which notably affects the El Gato diorite and the El Palofierrall orthogneiss. The migmatites occur as medium- to fine-grained rocks with well-developed banding of melanosome and leucosome (Figure 3d). The melanosome is generally composed of biotite, plagioclase, hornblende and orthopyroxene, and the leucosome includes quartz, plagioclase, K-feldspar, muscovite, biotite, clinopyroxene and titanite. Some of the observed migmatitic structures include patch, veins, stromatic and pygmatic folds, boudins, schlieren, nebulitic and net-like structures. There are also meter-scale outcrops of foliated to non-foliated amphibolite and diorite that display stromatic, brecciated, and dilatational-type structures characteristic of metatexites (Sawyer, 2008).

El Pajarito granite

This is a leucocratic, saccaroid-textured, medium-grained pluton with quartz phenocrysts that crops out in the southern part of the Sierra El Pajarito (Figures 2, 3c). To the north, El Pajarito pluton intrudes the El Gato diorite and is in turn cut by up to 2.5 m thick dikes of pegmatite and aplite, and by less than 1-cm thick veinlets of quartz with muscovite, pyrite and garnet. Petrographically this rock is holocrystalline and hypidiomorphic, mainly composed of quartz, microcline, and plagioclase (An_{15-25}), subordinate biotite and opaques; accessory minerals include pyroxene, garnet and zircon. K-feldspar

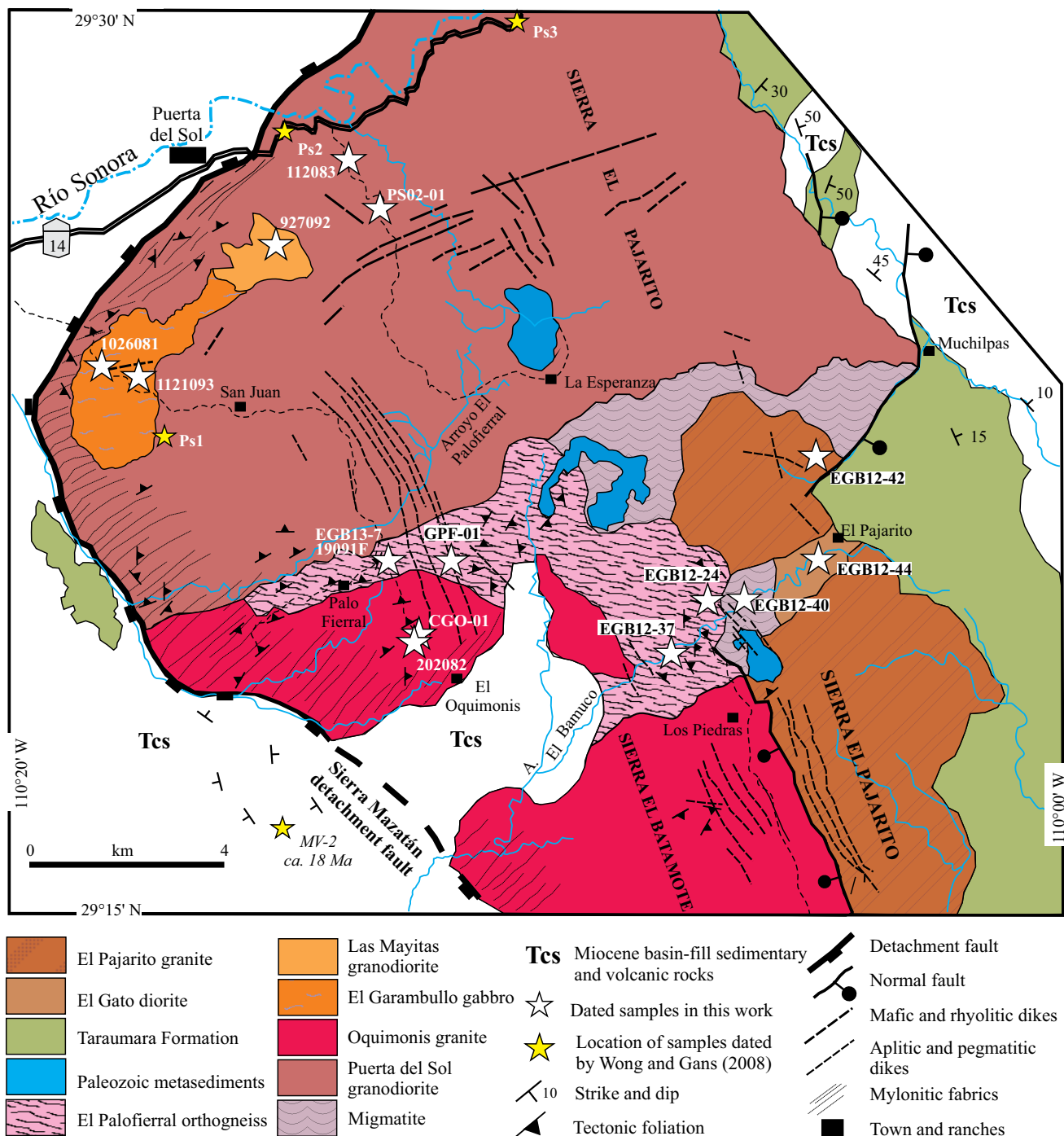


Figure 2. Geologic map of the Puerta del Sol area. Simplified from cartography to the scale 1:50,000 by González Becuar (2013).

crystals are subhedral and quartz tends to be subhedral to rounded with parallel extinction. Plagioclase crystals are euhedral and exhibit incipient to moderate alteration to muscovite + sericite, while biotite occurs as euhedral crystals with occasional muscovite and pyrite crystals along cleavage planes.

Puerta del Sol granodiorite

Outcrops of the Puerta del Sol granodiorite occupy most of the northern part of the study area (Figure 2). This pluton is mesocratic to leucocratic, medium- to coarse-grained, with well-defined magmatic

foliation indicated by the parallel alignment of 2 to 5 cm-long K-feldspar phenocrysts (Figure 3e). Its mineralogy consists of quartz + K-feldspar + plagioclase (An_{30-50}) + biotite + titanite + zircon. Quartz crystals are xenomorphic, commonly with undulose extinction, and K-feldspar occurs as orthoclase and less commonly microcline; plagioclase crystals are euhedral to subhedral with common oscillatory zoning. Biotite is anhedral to subhedral with moderate chloritization, and titanite crystals are rhombic, euhedral with skeletal structure. Incipient sericitic alteration is observed in feldspars, and propylitic alteration is observed as veinlets of chlorite and epidote. Proto-mylonitic to mylonitic

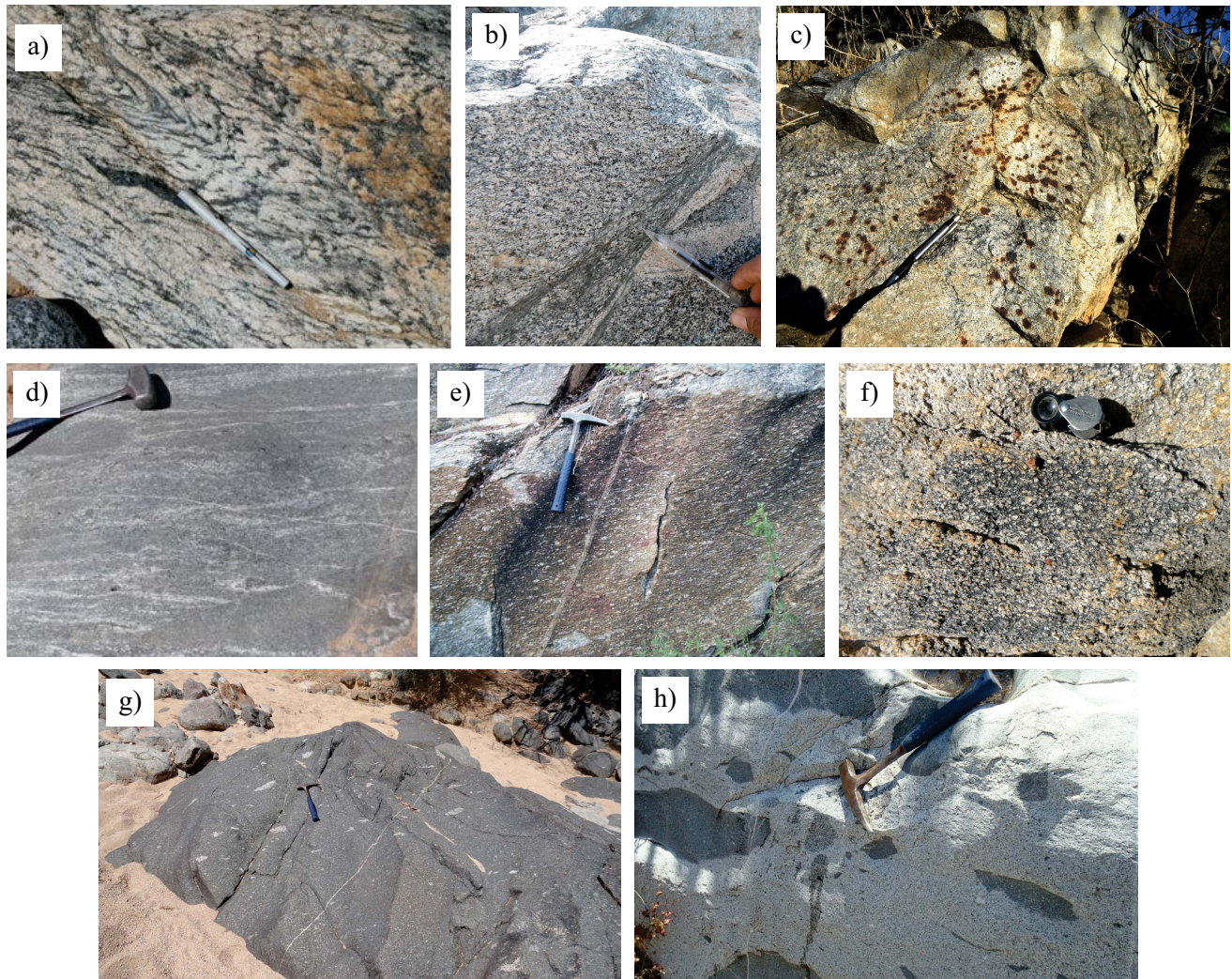


Figure 3. Field outcrop photographs of units outcropping in the Puerta del Sol area. a) The El Palofierral orthogneiss showing isoclinal folding in the Cañada El Bamuco. b) The El Gato diorite showing a porphyritic texture with local cataclastic banding. c) The El Pajarito granite displaying a leucocratic medium-grained, saccaroid texture with large crystals of oxidized pyrite. d) Stromatic migmatite with subparallel leucocratic lenses in a *schlieren*-like structure. e) The Puerta del Sol granodiorite with large K-feldspar phenocrysts aligned parallel to magmatic foliation. f) The leucocratic, medium- to coarse-grained Oquimonis granite with K-feldspar phenocrysts, quartz, muscovite and garnet. g) Outcrop of the El Garambullo gabbro showing aligned enclaves of granodioritic composition, most probably derived from the Puerta del Sol granodiorite. h) The Las Mayitas granodiorite with aligned mafic enclaves probably derived from the El Garambullo gabbro.

foliation is restricted to a ~1 km-wide zone along the westernmost part of the Puerta del Sol granodiorite outcrop (Figure 2), recording ductile deformation imprinted by the low-angle detachment fault that exhumed the crystalline rocks in the footwall.

El Oquimonis granite

The medium- to coarse-grained, leucocratic El Oquimonis granite crops out in the southern part of the quadrangle, where it forms the Sierra El Batamote (Figure 2). This pluton intrudes the El Palofierral orthogneiss and the Puerta del Sol granodiorite and is in sharp contact with the El Pajarito granite through a high-angle normal fault. The lithology corresponds to a two-mica granite composed of quartz, feldspar, muscovite, biotite and garnet (Figure 3f). Quartz crystals are commonly anhedral, with undulose extinction, and myrmekitic intergrowths with feldspars. K-feldspars are subhedral to euhedral orthoclase and microcline, while plagioclase is albite-oligoclase (An_{10-20}). Subordinate minerals consist of euhedral muscovite and biotite, and the accessory minerals are garnet crystals up to 1 cm long, fine-grained

apatite, zircon and opaque minerals. Slight to moderate sericitic alteration is observed in feldspar, while chloritic alteration occurs in biotite.

The western part of this pluton also records the heterogeneous proto-mylonitic foliation caused by shearing along the low-angle Sierra de Mazatán detachment fault, which place El Oquimonis granite in tectonic contact with clastic and volcanic deposits that form the upper plate of the metamorphic core complex.

El Garambullo gabbro

The El Garambullo gabbro is a melanocratic pluton that crops out in an area of ~20 km² (Figure 2), and intrudes the western part of the Puerta del Sol granodiorite. It is a fine- to medium-grained, equigranular to porphyritic rock consisting of plagioclase (An_{60-70}) + hornblende + opaque minerals + biotite + orthopyroxene, with common glomeroporphyritic association of hornblende + opaque minerals. Plagioclase (labradorite-bytownite) forms a crystalline groundmass of euhedral crystals over which hornblende phenocrysts grow. Hornblende includes disseminated opaque minerals (magnetite-

ilmenite) and is moderately to strongly altered to chlorite, epidote and actinolite. Biotite crystals are euhedral to subhedral with moderate chloritic alteration, and with opaque mineral inclusions along cleavage planes. Orthopyroxene (enstatite) is subrounded and associated with Fe-Mg minerals. Subordinate minerals are fine-grained, euhedral and disseminated rutile, spinel, apatite and zircon.

This pluton has local *schlieren*-like cumulates of ferromagnesian minerals, and mylonitic xenoliths from the Puerta del Sol granodiorite (Figure 3g) near the contacts. It also contains 2 to 20 cm-long aligned enclaves of gabbro and hornblende that define a magmatic foliation, as well as fragmented syn-plutonic mafic dikes. A few, up to 10 m-long darker gabbro enclaves are also recognized.

Las Mayitas granodiorite

This is a small pluton that forms a ~7 km² outcrop in the north-central part of the study area (Figure 2). It intrudes the Puerta del Sol granodiorite along a sharp contact, while its contact with the El Garambullo gabbro is a mingling zone (Figures 3h). This pluton consists of a fine-grained, mesocratic rock with quartz and plagioclase phenocrysts. The texture is hypidiomorphic and mineralogically consists of quartz, plagioclase (An₂₅₋₃₅) and orthoclase with subordinate biotite and accessory titanite, iron oxide and zircon. Plagioclase crystals are euhedral and occasionally glomeroporphyritic, whereas orthoclase has compositional zonation. Phenocrystic quartz is subhedral to anhedral, and it also fills spaces between feldspar crystals. The contact between the Las Mayitas and El Garambullo plutons is a diffuse zone that includes abundant aligned enclaves derived from both plutons developing flame and schlieren structures. These magmatic structures and fabrics occur in both plutons without evidence of magma mixing.

Dikes

Pegmatitic and aplitic dikes occur in the central and southeastern parts of the area (Figure 2) forming parallel dike swarms with a NW15-30° trend. They are composed of quartz, orthoclase, plagioclase, muscovite, biotite, and garnet, with thicknesses ranging from 5 to 120 cm, and intrude the El Oquimonis and the Puerta del Sol plutons. According to their field relationships they might be genetically related to the El Oquimonis granite, which is the younger rock they intrude.

A second, younger, prominent swarm of basaltic dikes cuts the Puerta del Sol granodiorite and the El Garambullo gabbro forming conspicuous NE- and NW-trending ridges in the northern part of the area (Radelli *et al.*, 1995; Bronner and Radelli, 1996; Wong and Gans, 2008). The mafic dikes dip 50°-70° SW and their thickness varies from 30 cm to 2 m. They are fine-grained rocks composed of plagioclase (An₇₀), hornblende, biotite, and opaque minerals. Scarcer, thinner dikes of rhyolitic composition that display parallel trends might be coeval to the mafic dikes forming a bimodal pulse. The rhyolitic dikes are porphyritic with crystals of quartz, K-feldspar and plagioclase up to 3 mm in size, along with accessory chloritized biotite in a fine, equigranular groundmass of quartz and feldspar. Wong and Gans (2008) dated one of the mafic dykes from outcrops along the Ures-Mazocahui highway and reported a ⁴⁰Ar/³⁹Ar hornblende age of 22.6 ± 0.4 Ma.

GEOCHEMISTRY

In order to geochemically characterize the different geologic events in the Puerta del Sol area, we analyzed 21 rock samples that were collected from fresh representative rock outcrops. Whole-rock samples were analyzed for major and trace elements (Table 1), while isotopic ratios of Sr, Nd and Pb were obtained in five samples (Table 2). Major elements were determined by X-ray fluorescence at Laboratorio

Universitario de Geoquímica Isotópica (LUGIS) of the Universidad Nacional Autónoma de México (UNAM), with a Rigaku Primus II 488 spectrometer, according to procedures described in Lozano-Santa Cruz and Bernal (2005). Trace element data were determined by ICP-MS at Laboratorio de Estudios Isotópicos, Centro de Geociencias, UNAM, using a Thermo ICap Q-ICPMS, and following the analytical techniques described in Mori *et al.* (2007). Isotopic ratios of Sr, Nd and Pb were determined at the Isotopic Laboratory of the University of Arizona, Department of Geosciences following procedures reported in appendix 4 of González-León *et al.* (2011) and at the University of Texas at Austin, according to procedure reported in appendix 1 of González-León *et al.* (2017).

Major and trace element geochemistry

The analyzed rock samples have loss on ignition (LOI) values ≤2.5 wt.% (Table 1), except for mafic dykes EGB12-38 and EGB12-39 that exceed that value and were only used for trace element interpretations. The concentration of major oxides was recalculated to 100% on an anhydrous basis and the results were plotted on classification diagrams to make geochemical interpretations.

A chemical classification of the rocks of the area based on the R1-R2 diagram of De la Roche *et al.* (1980) is consistent with the petrographic classification (Figure 4a). Two samples of the El Palofierral orthogneiss classify near the boundary between monzogranite and granodiorite and two samples of the El Gato pluton range from diorite to gabbrodiorite. Two leucosome migmatites classify as granodiorite and monzodiorite and a third sample from a melanosome is a syenogabbro. Two samples from the El Pajarito granite classify as monzogranite and syenogranite, three other from Puerta del Sol plot in the granodiorite field and four samples from the El Oquimonis granite plot closely as syenogranite, monzogranite and granodiorite. Two samples from the El Garambullo pluton plot as olivine gabbro, and a third sample classifies as a syenogabbro, while a single sample from the Las Mayitas plots as granodiorite.

The Laramide plutons have silica contents ranging from 55 to 76 wt. %. Silica variation diagrams of the major oxides show a general negative correlation with SiO₂, with the exception of Na₂O which displays a negligible positive correlation. All samples are subalkaline in a total alkali vs. silica diagram (Irvine and Baragar, 1971; Le Bas *et al.*, 1986). The AFM diagram (Irvine and Baragar, 1971) (Figure 4b) indicates calc-alkaline compositions, but one migmatite sample straddles the boundary to tholeiitic field. The SiO₂-K₂O diagram (Figure 4c) with discriminating fields of Peccerillo and Taylor (1976) indicates that the El Palofierral orthogneiss and the Laramide plutons are mostly high-K in composition except for the Puerta del Sol and El Gato plutons that plot as medium-K, close to the boundary with the high-K field. One of the migmatite samples is shoshonitic and the syn-extensional El Garambullo and Las Mayitas plutons plot also in the high-K and shoshonitic field.

In the alkali index diagram (Shand, 1943) (Figure 4d), the El Pajarito, the Puerta del Sol and Las Mayitas plutons are weakly peraluminous with Al₂O₃/(CaO+K₂O) molar ratios between 1 and 1.1. The El Oquimonis granite is clearly peraluminous, and the El Gato and El Garambullo plutons are metaluminous. Two of the migmatite samples are weakly peraluminous while a third sample is metaluminous. The Rb vs. (Y+Nb) tectonic discrimination diagram of Pearce *et al.* (1984; Figure 4e) shows that all of studied samples plot in the field of volcanic-arc granites.

Rare earth elements (REE) abundance of the studied samples were normalized to chondrite values (McDonough and Sun, 1995) and the resulting diagrams are shown in Figure 5. The Laramide plutons show an overall enrichment in light REE (LREE) with a negligible depletion in heavy REE (HREE), except for the leucocratic El Oquimonis and El

Table 1. Major (in wt. % oxide) and trace element (in ppm) data for metamorphic and magmatic rocks from the Puerta del Sol area.

Rock	El Palofieral orthogneiss		El Gato diorite		Migmatites		El Pajarito granite		Puerta del Sol granodiorite			El Oquimónis granite			Las Mayitas Granodiorite		El Garambullo gabbro		Mafic dikes	
	EGBI2-33	EGBI4-7	EGBI2-23	EGBI4-9	EGBI4-10	EGBI2-41	EGBI2-16	EP15-2	EP15-3	72509-1G	72509-3G	11208-3G	020208-2G	72509-3G	72409-1G	72509-2G	72409-2G	41808-1	EGBI2-38	EGBI2-39
Sample	EGBI2-33	EGBI4-7	EGBI2-23	EGBI4-9	EGBI4-10	EGBI2-41	EGBI2-16	EP15-2	EP15-3	72509-1G	72509-3G	11208-3G	020208-2G	72509-3G	72409-1G	72509-2G	72409-2G	41808-1	EGBI2-38	EGBI2-39
X	3246,793	3245,669	3243,978	3243,644	3244,442	3254,012	3236,280	3236,186	3258,358	3255,534	3251,139	3244,858	3248,570	3248,570	3248,570	3255,213	3254,126	3252,777	3251,838	3256,923
Y	576,052	573,213	588,140	585,617	584,332	585,991	587,059	590,720	590,609	573,583	571,550	571,479	576,850	575,134	575,134	586,544	572,544	568,949	567,450	570,026
SiO ₂	72.3	67.9	53.8	59.1	45.8	54.1	66.7	74.2	75.6	67.5	67.5	68.4	70.3	72.3	75.3	76.3	66.9	47.8	48.7	48.7
Al ₂ O ₃	15.0	16.0	21.5	17.2	19.5	19.2	16.9	13.5	13.4	17.1	15.1	15.5	15.8	15.3	14.6	14.0	16.2	17.8	17.9	15.1
Fe ₂ O ₃	2.4	3.8	6.0	6.9	11.9	8.9	3.0	1.2	1.1	3.2	2.2	1.0	2.8	2.2	0.7	0.4	3.3	10.6	8.3	9.8
CaO	1.7	3.0	7.1	5.6	8.3	6.3	2.5	0.8	0.7	3.7	2.5	1.2	2.7	2.4	1.1	0.6	2.8	7.5	8.7	6.9
Na ₂ O	3.0	4.1	4.2	3.7	3.4	3.5	4.2	3.7	4.3	4.7	3.8	4.2	4.3	4.3	3.9	3.6	3.9	3.6	2.9	2.0
K ₂ O	5.0	3.6	1.6	1.8	1.8	1.8	4.2	5.1	4.1	2.4	2.8	3.8	3.2	3.0	4.2	4.8	3.9	3.1	1.4	1.7
MgO	0.3	1.0	2.1	2.4	4.7	3.3	1.0	0.1	0.1	0.8	0.5	0.0	0.7	0.6	0.2	0.0	1.4	5.5	7.2	9.6
TiO ₂	0.3	0.7	0.9	0.9	1.5	1.3	0.4	0.0	0.0	0.4	0.3	0.1	0.3	0.3	0.1	0.0	0.5	1.4	1.1	1.4
P ₂ O ₅	0.1	0.3	0.2	0.3	0.5	0.3	0.1	0.0	0.0	0.2	0.1	0.0	0.1	0.1	0.0	0.0	0.2	1.1	0.4	0.6
MnO	0.0	0.1	0.1	0.1	0.2	0.1	0.1	0.0	0.1	0.1	0.1	0.0	0.1	0.1	0.0	0.0	0.1	0.2	0.1	0.2
LOI	0.7	1.2	1.6	1.7	2.2	0.9	0.4	0.3	0.2	0.7	0.5	0.4	0.5	0.3	0.3	0.3	0.5	1.7	2.5	5.5
Total	100.8	101.9	99.2	99.8	99.9	99.8	99.3	99.0	99.7	100.9	95.3	94.7	100.8	100.8	100.5	100.1	99.6	100.2	99.2	100.4
Cs	2.1	3.4	7.1	3.0	1.6	1.2	-	0.7	1.3	0.6	-	-	-	1.6	1.9	-	0.6	1.3	-	1.6
Rb	139.6	145.5	78.5	77.3	65.5	51.1	88.7	153.5	214.0	66.0	96.0	113.0	95.0	94.0	126.0	212.9	59.3	71.0	38.0	45.4
Ba	1,291.8	2,120.0	753.4	640.0	807.0	809.1	120.0	100.5	36.2	-	1,216.0	1,048.0	1,227.0	1,091.0	817.0	67.6	688.9	1192.0	885.0	749.0
Th	16.5	6.7	8.1	7.3	0.9	2.3	-	12.6	12.2	9.8	10.0	7.0	9.2	9.7	3.7	3.5	5.2	4.0	10.0	2.6
U	2.1	1.7	3.6	3.3	0.6	0.3	12.7	5.7	4.7	2.3	-	-	-	1.2	0.7	12.1	1.0	1.8	-	0.5
Nb	13.2	13.1	13.3	12.4	11.4	7.4	34.5	24.1	21.1	10.0	15.0	9.0	9.0	7.0	4.0	5.8	7.2	12.0	7.0	12.2
Ta	0.7	0.8	1.5	1.1	0.5	0.4	-	1.6	1.7	1.3	-	-	-	0.5	0.6	0.4	0.6	0.6	-	0.6
Pb	23.3	11.0	10.8	6.0	6.0	6.4	18.1	28.0	27.0	11.9	17.0	20.0	11.5	14.2	21.0	21.2	7.3	11.0	7.2	6.4
Sr	209.8	575.0	658.5	553.0	760.0	718.1	545.8	46.4	34.2	571.0	565.0	338.0	467.0	449.0	218.0	52.6	376.1	1,679.0	1,977.0	668.9
Zr	9.6	332.0	385.3	176.0	254.0	14.7	198.7	43.0	46.0	261.0	230.0	82.0	233.0	239.0	72.0	47.5	118.6	262.0	243.0	50.2
Y	14.4	15.6	26.3	29.1	35.2	19.4	15.7	30.9	27.9	20.0	6.8	18.0	9.7	17.0	25.0	26.0	8.6	33.0	20.0	27.7
Hf	0.1	8.5	8.4	4.8	5.7	0.6	5.0	2.3	2.8	0.4	6.5	2.5	0.3	0.6	0.2	2.5	3.1	1.3	2.4	4.1
La	51.3	49.6	22.9	36.3	21.3	20.7	34.5	7.6	6.5	44.0	34.5	17.0	40.6	31.0	7.9	5.8	25.7	197.3	32.6	35.0
Ce	101.3	103.0	45.7	75.9	56.1	43.2	67.5	16.3	14.4	82.1	64.9	31.7	74.2	55.3	15.1	12.1	44.9	395.3	73.9	73.4
Pr	11.7	12.2	6.4	9.0	8.0	5.7	7.7	2.0	1.8	9.6	6.8	3.7	8.4	5.9	1.7	1.5	5.1	23.4	9.9	9.5
Nd	40.2	45.0	24.3	32.8	34.5	23.7	26.6	9.3	8.3	34.5	23.2	13.5	28.5	20.3	6.5	5.9	17.2	90.7	42.0	37.6
Sm	6.2	8.5	4.9	6.5	8.0	5.2	4.4	3.0	2.9	6.1	3.6	2.5	4.2	3.2	1.5	1.9	2.8	14.8	7.9	7.5
Eu	1.4	2.0	1.5	1.5	2.1	1.4	1.1	0.3	0.2	1.1	0.9	0.4	0.7	0.6	0.3	0.2	0.6	3.1	2.2	1.9
Gd	4.4	5.7	4.4	6.0	7.8	4.7	3.4	3.9	3.2	5.1	2.7	2.4	3.0	2.8	1.8	2.7	2.2	11.8	5.8	6.5
Tb	0.6	0.7	0.7	0.9	1.2	0.7	0.5	0.8	0.7	0.7	0.4	0.3	0.4	0.4	0.4	0.6	0.3	1.4	0.7	0.9
Dy	2.8	3.5	4.1	5.5	7.1	3.8	2.6	5.3	4.6	3.7	1.6	2.0	1.7	1.7	2.2	4.0	1.4	6.2	4.0	5.1
Ho	0.5	0.5	0.9	1.0	1.4	0.7	0.5	1.2	0.9	0.7	0.3	0.4	0.3	0.3	0.5	0.8	0.3	1.2	0.7	1.0
Er	1.4	1.3	2.6	2.9	3.7	1.8	1.5	3.4	2.8	1.8	0.7	1.1	0.8	0.7	1.4	2.4	0.9	2.8	1.8	2.6
Yb	1.0	1.0	3.0	2.8	3.1	1.3	2.6	3.7	3.0	1.7	0.5	1.0	0.7	0.7	1.2	2.3	0.8	2.6	1.5	2.3
Lu	0.2	0.1	0.5	0.4	0.5	0.2	0.3	0.5	0.4	0.2	0.1	0.1	0.1	0.1	0.2	0.3	0.1	0.4	0.2	0.3
Tm	-	-	-	-	-	-	-	0.5	0.4	0.3	0.1	0.2	0.1	0.1	0.1	0.2	-	0.4	0.3	-

Table 2. Isotopic composition of selected plutonic and metamorphic rocks from the Puerta del Sol area.

Sample	EGB12-33	EGB12-23	7-25-09-3	9-27-09-2	11-21-09-3
Unit	El Paloferal orthogneiss	El Gato diorite	El Oquimonis granite	Las Mayitas granodiorite	El Garambullo gabbro
Age (Ma)		72	42	20	20
Sm (ppm)		3.69	4.67	5.08	8.75
Nd (ppm)		19.02	30.38	33.81	47.34
$^{147}\text{Sm}/^{144}\text{Nd}$		0.117377	0.092945	0.090883	0.111743
$^{143}\text{Nd}/^{144}\text{Nd}(0)$		0.512204	0.512476	0.512419	0.512397
std error (%)		0.0051	0.0015	0.0014	0.0010
$^{143}\text{Nd}/^{144}\text{Nd}(i)$		0.512149	0.512450	0.512407	0.512382
$\epsilon(\text{Nd})0$		-8.46	-3.16	-4.27	-4.70
$\epsilon(\text{Nd})i$		-7.73	-2.60	-4.00	-4.48
Rb (ppm)		78.47	84.89	99.37	26.93
Sr (ppm)		658.48	521.63	566.94	1,374.36
$^{87}\text{Rb}/^{86}\text{Sr}$		0.345098	0.468555	0.503998	0.056342
$^{87}\text{Sr}/^{86}\text{Sr}(0)$		0.709295	0.708255	0.707047	0.707260
std error (%)		0.0061	0.0022	0.0021	0.0021
$^{87}\text{Sr}/^{86}\text{Sr}(i)$		0.708942	0.707975	0.706904	0.707244
$^{206}\text{Pb}/^{204}\text{Pb}$	19.4081	19.2255	19.2643	19.1046	19.0911
$^{207}\text{Pb}/^{204}\text{Pb}$	15.6796	15.6557	15.6842	15.6562	15.6663
$^{208}\text{Pb}/^{204}\text{Pb}$	38.7306	38.6994	38.8977	38.7810	38.7825

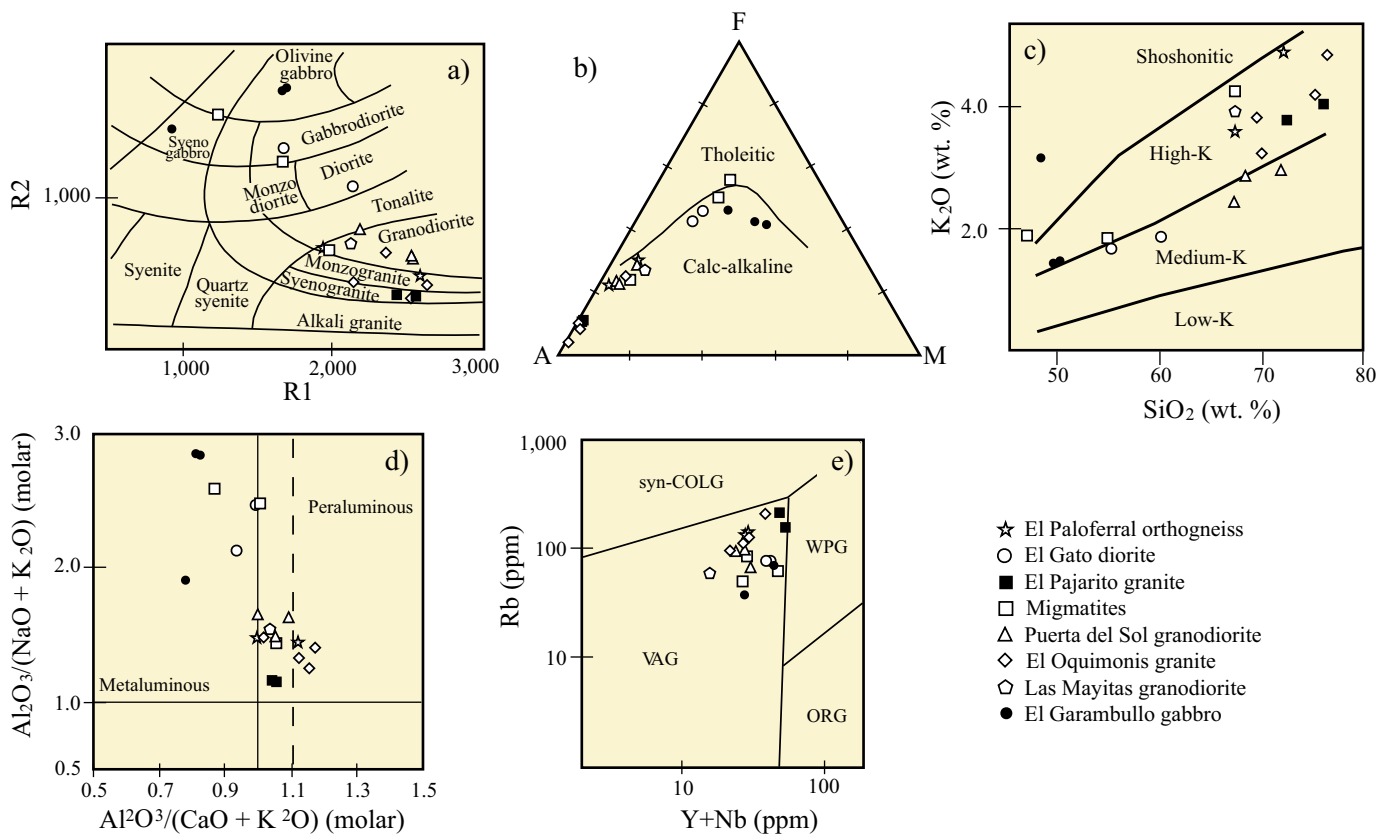


Figure 4. Geochemical discrimination plots for the plutons of the Puerta del Sol area. a) Chemical classification of the rocks based on the R1-R2 diagram of De La Roche *et al.* (1980). R1 and R2 parameters express equations in milicatic proportions: $R1 = 4\text{Si} - 11(\text{Na} + \text{K}) - 2(\text{Fe} + \text{Ti})$; $R2 = 6\text{Ca} + 2\text{Mg} + \text{Al}$. b) AFM ternary diagram including the discrimination line from Kuno (1968), A: $\text{Na}_2\text{O} + \text{K}_2\text{O}$; F: Total FeO; M: MgO. c) K_2O vs. SiO_2 diagram with K fields of Peccerillo and Taylor (1976). d) Discrimination diagram based on the Shand index in molar proportions. Stippled line on the vertical axis marks the boundary between slight to high peraluminous fields from Chappel and White (1974). e) Pearce *et al.* (1984) tectonic discrimination diagram showing the composition of the studied plutons: VAG (volcanic arc granite), syn-COLG (syn-collisional granites), WPG (within-plate granites), ORG (oceanic ridge granites).

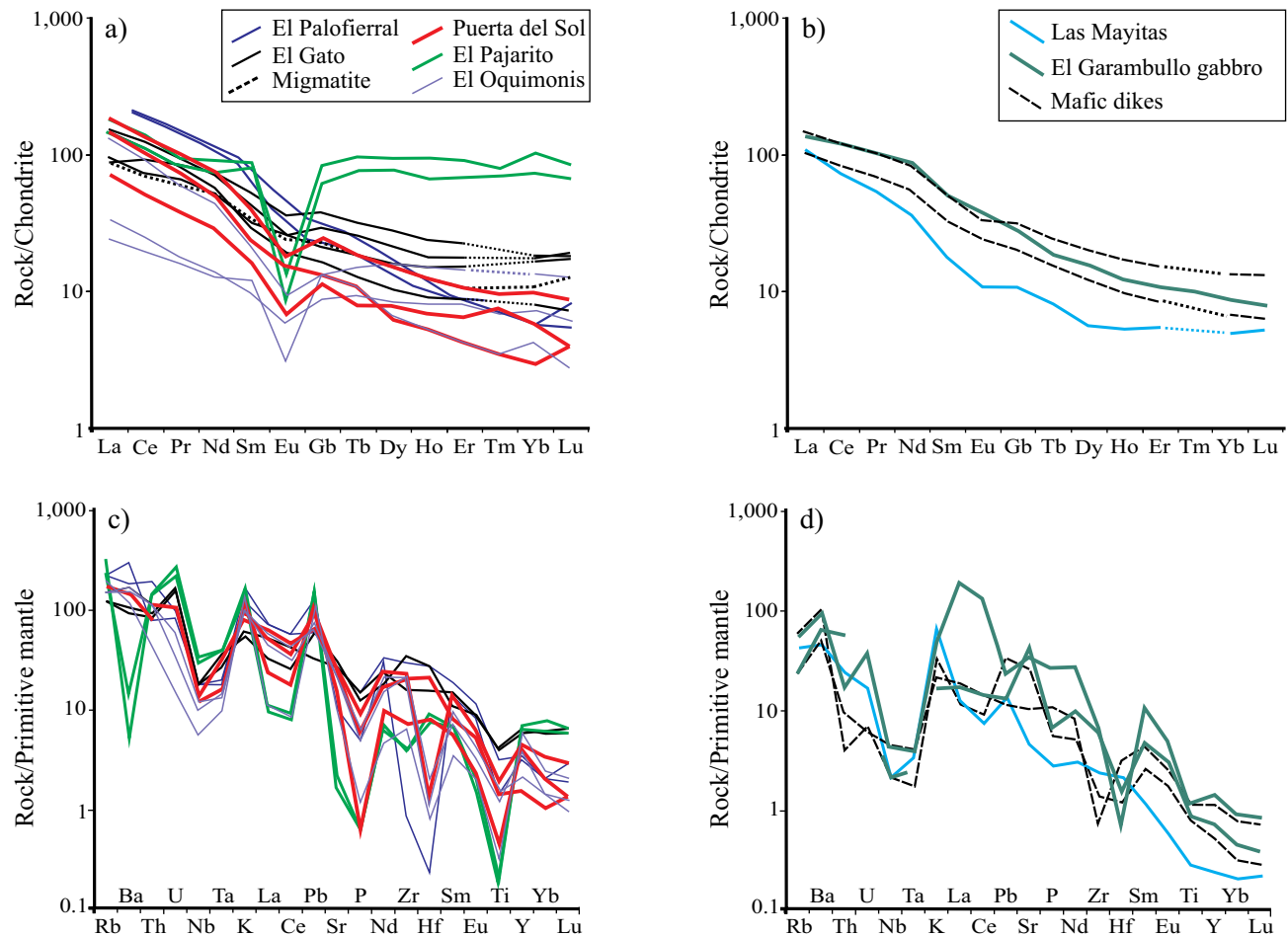


Figure 5. Chondrite-normalized rare earth element (REE) diagrams for a) the Laramide plutons of the area, including the El Palofierral orthogneiss, and b) the Miocene syn-extensional El Garambullo gabbro and Las Mayitas granodiorite and the mafic dykes. Primitive mantle-normalized multi-element diagrams for (c) the Laramide plutons of the study area, and (d) the Miocene syn-extensional plutons and the mafic dykes. Normalization values are from McDonough and Sun (1995) in a) and b), and from Sun and McDonough (1989) for diagrams in c) and d).

Pajarito plutons that have different REE patterns. Two samples from the El Oquimonis granite show the lowest LREE values (Figures 5a), while two samples from the El Pajarito granite show overall flat REE patterns. The El Oquimonis and El Pajarito intrusives also have pronounced negative Eu anomalies and the Puerta del Sol granodiorite tends to mimic this pattern but with a less negative Eu anomaly. REE diagrams for the El Garambullo gabbro and the mafic dikes show nearly similar patterns with enrichment in LREE and depletion of the HREE, which display nearly flat curves. The Las Mayitas granodiorite follows a nearly similar trend than the mafic rocks but at relatively lower total REE content.

Multielemental diagrams normalized to primitive mantle values (Sun and McDonough, 1989) display nearly similar jagged patterns (Figure 5c, 5d). They show relative enrichment in K, Rb, Ba and Pb compared to Hf, Zr and Y. The El Pajarito granite however has very low values in Ba. They also show negative anomalies for Nb-Ta (Figures 5c), Sr, P and Ti. The syn-extensional plutons and mafic dikes nearly follow the same elemental pattern (Figure 5d).

Isotope geochemistry

Isotope ratios of Sr, Nd and Pb were obtained in samples from El Gato diorite, El Oquimonis granite, Las Mayitas granodiorite and El Garambullo gabbro, and Pb isotopes values were obtained for the El

Palofierral orthogneiss (Table 2). The initial $^{87}\text{Sr}/^{86}\text{Sr}$ ratios for these plutons range from 0.7069 to 0.7089 and their initial ϵNd values from -2.6 to -7.7 (Table 2). Their $^{206}\text{Pb}/^{204}\text{Pb}$ ratios range from 19.09 to 19.26, the $^{207}\text{Pb}/^{204}\text{Pb}$ ratios from 15.65 to 15.68, and the $^{208}\text{Pb}/^{204}\text{Pb}$ ratios from 38.69 to 38.89. The $^{206}\text{Pb}/^{204}\text{Pb}$, $^{207}\text{Pb}/^{204}\text{Pb}$ and $^{208}\text{Pb}/^{204}\text{Pb}$ ratios for the El Palofierral orthogneiss are 19.48, 15.67, and 38.73, respectively. The composition of these rocks is plotted in Figure 6, and compared with similar data reported for Paleoproterozoic and Laramide plutonic rocks from neighboring areas of central Sonora.

GEOCHRONOLOGY

Ages of the magmatic events that occurred in the Puerta del Sol area are constrained by nine U-Pb, five K-Ar and two $^{40}\text{Ar}/^{39}\text{Ar}$ ages (Table 3). U-Pb zircon ages were obtained by laser ablation inductively-coupled plasma mass spectrometry (LA-ICPMS) in the Centro de Geociencias, UNAM following procedures described in Solari *et al.* (2010, 2015) [results are reported in Supplemental Table A], and by laser ablation-multicollector-inductively coupled plasma-mass spectrometry (LA-MC-ICP-MS) at the Arizona LaserChron Center of the Department of Geosciences, University of Arizona, using the procedures described by Gehrels *et al.* (2006) [results are reported in

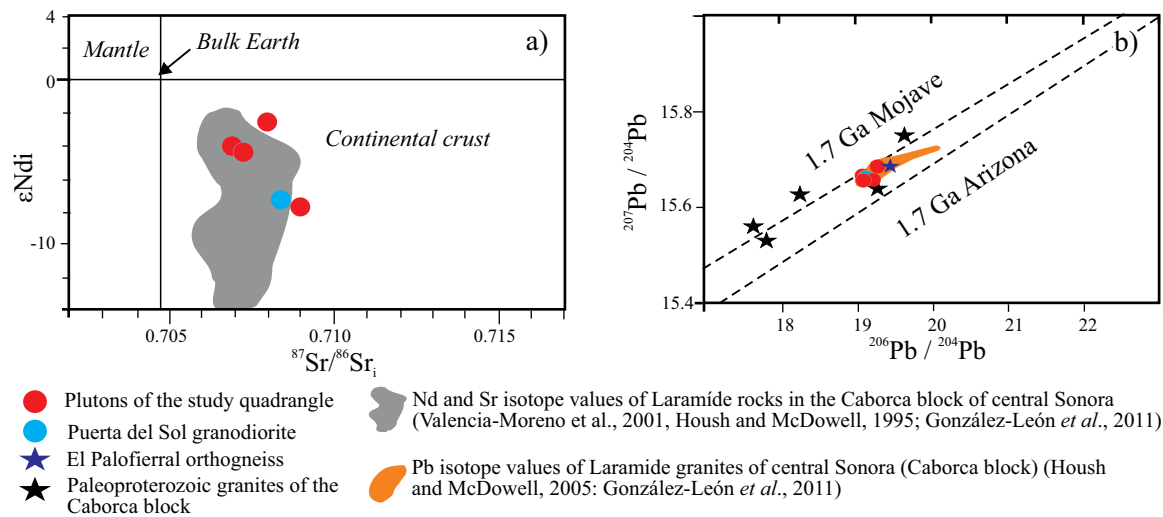


Figure 6. a) Plot of initial ϵ_{Nd} versus $^{87}Sr/^{86}Sr$ values for the El Gato, El Oquimonis, Las Mayitas and El Garambullo plutons of the Puerta del Sol area. Values plot close to the Laramide granites of the Caborca block in central Sonora (gray field) reported by other authors and summarized in González-León *et al.* (2011). Sr and Nd values of the Puerta del Sol granodiorite (blue dot) are from González-León *et al.* (2011) b) Uranogenic diagram (Wooden *et al.*, 1988; Wooden and DeWitt, 1991) showing plots of the El Palofierral orthogneiss and the Laramide and syn-extensional plutons of the study area. Black stars are Pb isotope values reported from Paleoproterozoic granites of the Caborca terrane by Farmer *et al.* (2005) and González-León *et al.* (2011).

Supplemental Table B]. K-Ar analyses were conducted at Instituto de Geología, UNAM, with the procedures described in appendix 3 of González-León *et al.* (2011). The $^{40}Ar/^{39}Ar$ dating was performed at Laboratorio de Geocronología of the Departamento de Geología, Centro de Investigación Científica y de Educación Superior de Ensenada (CICESE), with procedures described in González-León *et al.* (2010).

U-Pb ages were determined in zircon separates for samples of the El Palofierral orthogneiss, El Gato diorite, El Pajarito granite, Puerta del Sol granodiorite, El Oquimonis granite, two different samples

of migmatites, and the Garambullo gabbro (see sample locations in Figure 2). One sample of the El Palofierral orthogneiss was collected from the El Bamuco creek (sample EGB12-24) and a second one from near rancho El Palofierral (sample EGB13-7). Zircons of these samples are euhedral to anhedral, with concentric zoning, and some display irregular metamorphic overgrowths. From sample EGB12-24 we measured 26 individual zircons in their rims and cores. The concordia diagram of Figure 7a indicates that the analyzed zircons describe a discordia line, with a Paleoproterozoic upper intercept and a Late Cretaceous lower intercept. The mean age of the zircons defining the

Table 3. Summary of U-Pb, K-Ar and Ar/Ar ages obtained for Puerta del Sol units.

Sample	Rock unit	UTM (12R)		Age (Ma)		
		E	N	U-Pb (z)	K-Ar	$^{40}Ar-^{39}Ar$
EGB12-24	El Palofierral orthogneiss	586,623	3'244,995	1,685 ± 15 66 ± 21 (rims)		
EGB13-7	El Palofierral orthogneiss			1672 ± 12 61.7 ± 4.1 (rims)		
EGB12-44	El Gato diorite	589,270	3'246,925	71.29 ± 0.45		
EGB12-42	El Pajarito granite	588,452	3'251,810	67.9 ± 0.43		
EGB12-37	Migmatite	586,630	3'244,988	1,683.9 ± 9.6 (cores): 64.3 ± 1.1 (rims)		
EGB12-40	Migmatite			58.91 ± 0.41		
112083	Puerta del Sol granodiorite	573,580	3'258,270	49.1 ± 0.46		
202082	Oquimonis granite	576,850	3'244,858	41.78 ± 0.32		
CGO-01	Oquimonis granite	576,670	3'244,830		26.3 ± 0.6 (mc)	
GPF-01	El Palofierral orthogneiss	576,052	3'246,793		23.2 ± 0.8 (bt)	
19091F	El Palofierral orthogneiss	575,140	3'246,040			23.0 ± 1.3 (kf)
CGO-01	Oquimonis granite	576,670	3'244,830		21.8 ± 0.5 (bt)	
PS02-01	Puerta del Sol granodiorite	576,120	3'255,318		20.2 ± 0.6 (bt)	
1121093	El Garambullo gabbro	568,679	3'251,838	19.83 ± 0.18		
927092	Las Mayitas granodiorite	573,835	3'255,437		19.2 ± 1.2 (bt)	
1026081	El Garambullo gabbro	568,300	3'252,016			17.4 ± 1.0 (pg)

Note: bt: biotite; kf: k-Feldspar; pg: plagioclase; mc: muscovite; z: zircon

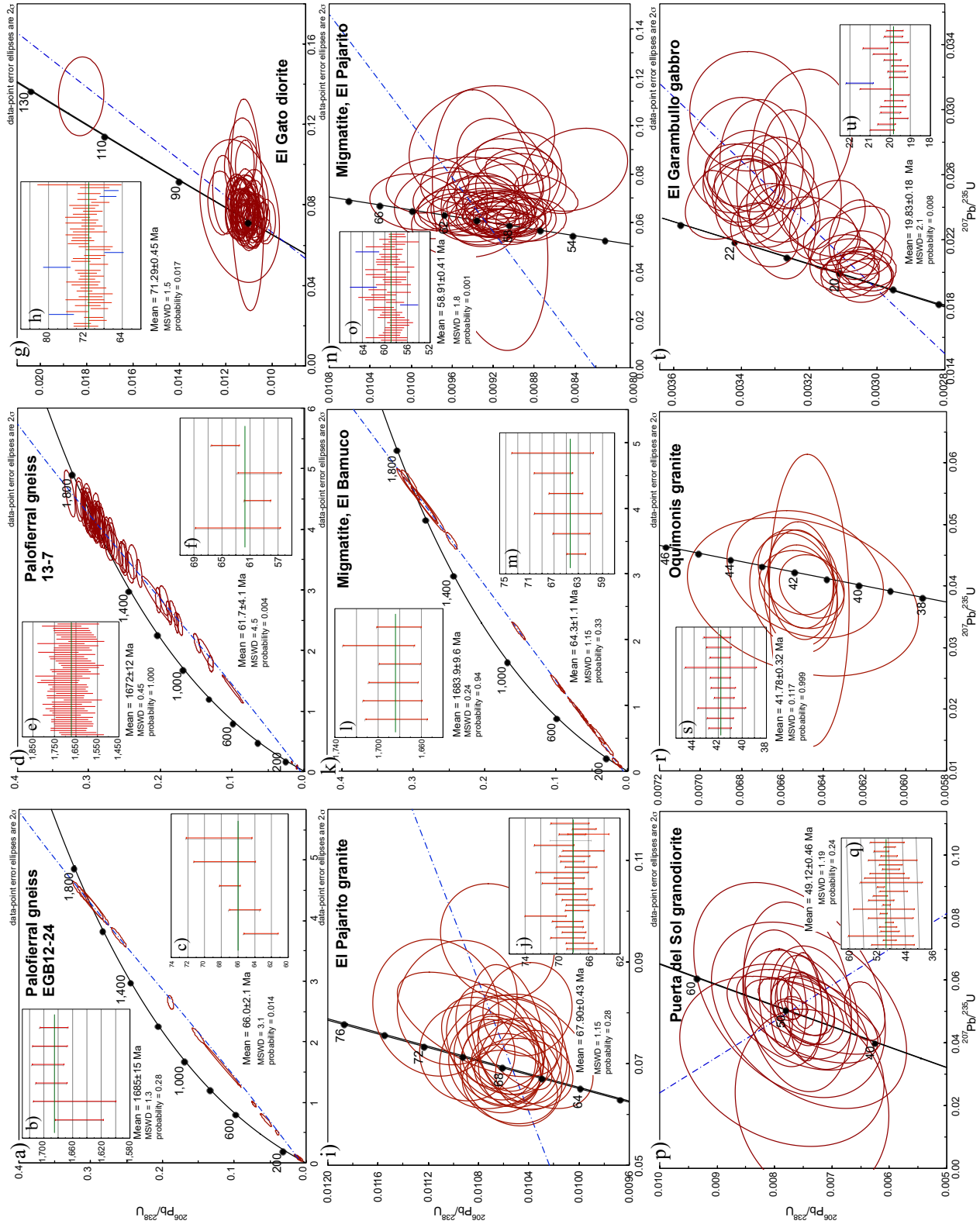


Figure 7. U-Pb ages for the rocks of the study quadrangle. a-c) Ages of sample EGB12-24 from the El Paloferrall orthogneiss obtained in cores (b) and in rim (c) of the dated zircons. d-f) Sample EGB13-7 from the El Paloferrall orthogneiss collected in rancho El Paloferrall: e) age of zircon cores and f) mean-age diagram. g-h) Sample EGB12-44 from the El Gato diorite: h) mean-age diagram. i-j) Sample EGB12-42 from the El Pajarito granite: i) mean-age diagram. k-m) Sample EGB12-37 from a migmatite: l) in zircon cores and m) in rims. n-o) Sample EGB12-40 from a migmatite: o) mean-age diagram. p-q) Sample 112083 from the Puerta del Sol granodiorite: q) mean-age diagram. r-s) Sample 202082 from El Oquimonis granite: s) mean-age diagram. t-u) Sample 1121093 from the El Garambullo gabbro: u) mean-age diagram.

upper intercept is of $1,685 \pm 15$ Ma (Figure 7b) and a younger population obtained from zircon rims yielded a mean age of 66 ± 2.1 Ma in a group of five zircons (Figure 7c). Sample EGB13-7 has a similar behavior, with a discordia (Figure 7d) that joins an upper intercept with a mean age of $1,672 \pm 12$ Ma (Figure 7e) in 52 measured zircons, and a lower intercept at a mean age of 61.7 ± 4.1 Ma (Figure 7f) obtained by analysis of zircon rims.

Sample EGB12-44 from the El Gato diorite yielded euhedral to subhedral, slender zircons with concentric zoning. All of them are concordant to slightly discordant (Figure 7g), with a mean age of 71.29 ± 0.45 Ma defined by a coherent group of 44 analyses (Figure 7h). The El Pajarito granite sample EGB12-42 yielded euhedral to subhedral, slender concordant zircons with concentric zoning and a mean age of 67.9 ± 0.43 Ma obtained from a coherent group of 19 zircons (Figures 7i and 7j).

Dated samples EGB12-37 and EGB12-40 were collected from migmatites that crop out along the El Bamuco creek. Sample EGB12-37 belongs to a foliated migmatitic amphibolite with stromatic leucosome bands that crop out within the El Palofierrall orthogneiss. It yielded euhedral to subhedral zircons with concentric zoning. The concordia diagram evidences upper and lower intercepts (Figure 7k). Six ages obtained from the zircon cores yielded a mean age of $1,683.9 \pm 9.6$ Ma (Figure 7l), whilst six ages from zircon rims yielded a mean age of 64.3 ± 1.1 Ma (Figure 7m). Sample EGB12-40 collected from a migmatite exposed near the El Gato pluton and near El Pajarito ranch yields concordant ages (Figure 7n) with a mean age of 58.91 ± 0.41 Ma in a group of 40 zircon rim analyses (Figure 7o).

Sample 112083 from the Puerta del Sol granodiorite yields concordant analyses (Figure 7p) with a mean age of 49.1 ± 0.46 Ma in a coherent group of 24 measured zircons (Figure 7q), while sample 202082 from the El Oquimonis granite also yielded concordant ages (Figure 7r) with a mean age of 41.78 ± 0.32 Ma in a group of ten zircons (Figure 7s). The youngest U-Pb age obtained was for sample 1121093 collected from El Garambullo gabbro that yielded concordant results (Figure 7t) with a mean age of 19.83 ± 0.18 Ma (Figure 7u) in a coherent group of nine out of 17 measured zircons.

We also obtained K-Ar ages for El Palofierrall orthogneiss, El Oquimonis granite, and Puerta del Sol and Las Mayitas granodiorites (Table 4). A biotite separated from sample GPF-01 from El Palofierrall orthogneiss gave an age of 23.2 ± 0.8 Ma and two ages obtained from sample CGO-01 from the El Oquimonis granite yielded ages at 26.3 ± 0.6 Ma in muscovite and at 21.8 ± 0.5 Ma in biotite. Also, sample PS02-01 from the Puerta del Sol granodiorite was dated at 20.2 ± 0.6 Ma in biotite, while sample 927092 from the Las Mayitas granodiorite was dated at 19.2 ± 1.2 Ma.

Two other samples, one collected from the El Palofierrall orthogneiss (19091F) and another one collected from the El Garambullo gabbro (1026081) were dated by the $^{40}\text{Ar}/^{39}\text{Ar}$ method. Sample 1909F1 reveals excess argon as suggested by the “U” shaped age spectrum (Figure 8a), the best age was obtained at the intercept with an isochron age of

23.0 ± 1.3 Ma in K-feldspar. Sample 1026081 yielded an acceptable plateau age of 17.4 ± 1.0 Ma in plagioclase (Figure 8b) for the El Garambullo gabbro.

DISCUSSION

The study area lies within the Proterozoic crustal Caborca block, far south of the boundary with the Mazatzal block (see inset map in Figure 1). This boundary, that juxtaposes both blocks, corresponds to the Jurassic Mojave-Sonora megashear as postulated by Anderson and Silver (2005). Arvizu *et al.* (2009) however suggested that a parallel strip of the Yavapai province (Bennet and DePaolo, 1987) separates the crustal Mazatzal and Caborca blocks in Sonora. They also assigned the Caborca block to the Paleoproterozoic Mojave province of southwestern North America, with U-Pb ages for the crystalline basement in Sonora of *ca.* 1.76 to 1.64 Ga (summarized in Iriondo and Premo, 2011). The age of *ca.* 1.68 Ga that we obtained for the El Palofierrall orthogneiss is within the age range assumed for the basement of the Caborca block and the obtained Pb isotope ratios plot close to the field of the Paleoproterozoic rocks of the Mojave province (Wooden *et al.*, 1988; Wooden and DeWitt, 1991) (Figure 6b), similarly to other Paleoproterozoic granitoids reported from the Caborca block in Sonora (Farmer *et al.*, 2005; González-León *et al.*, 2011). In Figure 6b, the El Palofierrall orthogneiss also plots within the field of values for Laramide granites emplaced in the Caborca block of central and southern Sonora (as compiled in González-León *et al.*, 2011), as observed for other plutonic rocks of the study quadrangle.

Laramide plutonism

The oldest Laramide plutonic event in the area is recorded by the intrusion of the El Gato diorite that occurred at 71.29 ± 0.45 Ma. The restricted outcrop of this pluton in the east-central part of the study area is separated from the El Palofierrall orthogneiss by a zone of migmatization that affects both units. In its eastern part, El Gato diorite intrudes undated rocks of the Tarahumara Formation. Volcanic rocks of the Tarahumara Formation from nearby areas of central Sonora have been dated between *ca.* 80 and 59 Ma (González-León *et al.*, 2011). The El Pajarito granite is a leucocratic, slightly peraluminous granite that intruded the El Gato diorite at ~ 68 Ma.

The migmatization event in the central part of the area affects rocks of El Gato diorite and El Palofierrall orthogneiss along the intrusive contact between both units. Far from this contact, local patches of migmatization also occur within the El Palofierrall orthogneiss (Figure 2). The migmatization event also affects the El Pajarito granite along its contact with the southern part of the El Gato diorite. The zone of migmatization occurring to the north of the El Pajarito granite and northeast of the El Palofierrall orthogneiss might be affecting these three plutonic bodies. Nevertheless, the migmatization event in the area is a complex event and should be better clarified by subsequent studies.

Table 4. Analytical data of K-Ar ages obtained for plutons of the Puerta del Sol area.

Sample	Rock Unit	Mineral	%K	$^{40}\text{Ar}^*$ (moles/g) $\times 10^{-10}$	% $^{40}\text{Ar}^*$	Age (Ma)
GPF-01	El Palofierrall orthogneiss	Biotite	7.49	3.03	49.1	23.2 ± 0.8
CGO-01	El Oquimonis granite	Biotite	7.65	2.906	89.1	21.8 ± 0.5
CGO-01	El Oquimonis granite	Muscovite	8.35	3.839	85	26.3 ± 0.6
PS02-01	Puerta del Sol granodiorite	Biotite	7.42	2.611	91.2	20.2 ± 0.6
927092	Las Mayitas granodiorite	Biotite	7.38	2.465	75.2	19.2 ± 1.2

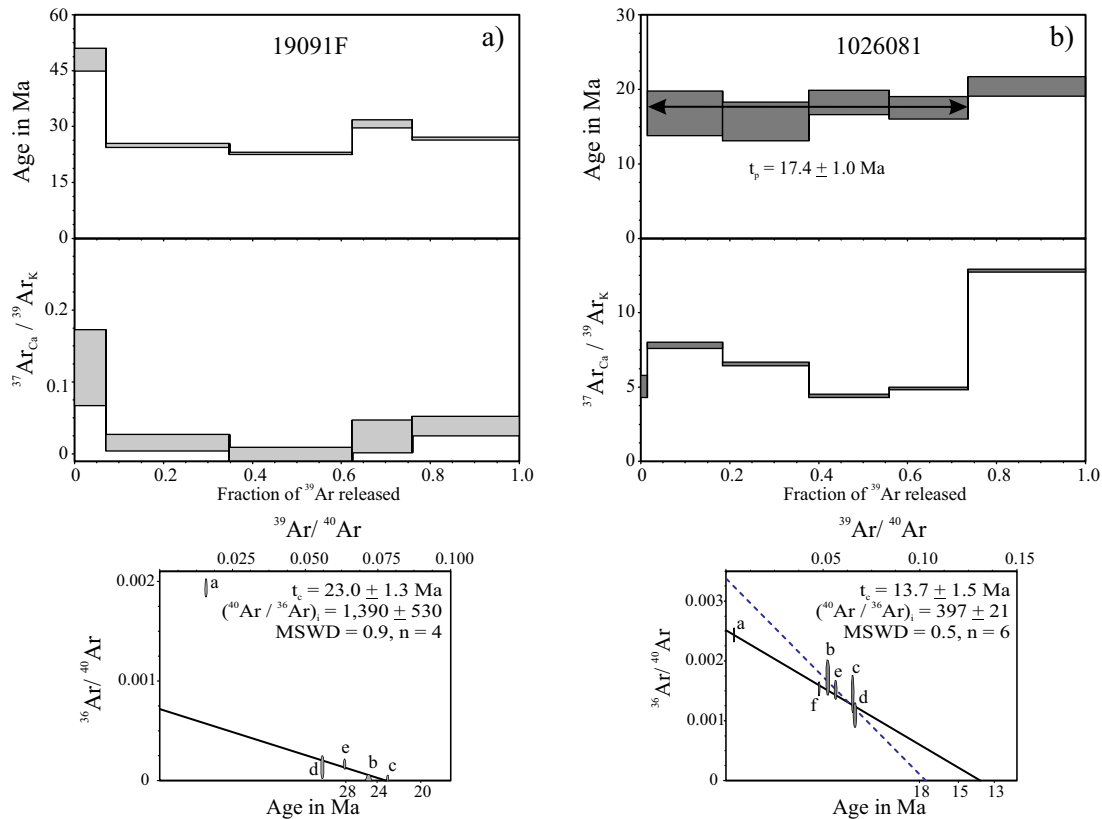


Figure 8. $^{40}\text{Ar}/^{39}\text{Ar}$ dating for (a) Sample 19091F from the El Palofierral orthogneiss and (b) sample 1026081 from the El Garambullo gabbro.

Zircon cores from a migmatitic amphibolite (sample EGB12-37) within the El Palofierral orthogneiss yielded inherited ages accordingly to the host rock, but ages of 64.3 ± 1.1 Ma were obtained for the zircon rims (Figure 7f). Another age obtained for a migmatite that affects the El Gato diorite (sample EGB12-40) was of 58.91 ± 0.41 Ma (Figure 7o). Furthermore, zircon rims dated from sample EGB12-24 and EGB13-7 of the El Palofierral orthogneiss yielded mean ages of 66 ± 2.1 Ma (Figure 7c) and 61.7 ± 4.1 Ma (Figure 7f), respectively. If the ages obtained from zircon rims of the El Palofierral orthogneiss are considered to be part of this event, and considering the error margins, they apparently indicate that migmatization occurred between ~ 68 and ~ 59 Ma, in a time slightly younger than emplacement of the El Pajarito granite (*ca.* 68 Ma). Consequently, the migmatization in the area might be tentatively assigned to partial melting related to thermal metamorphism resulting from a contemporaneous deep-seated plutonic intrusion in the area. This pluton might be the El Pajarito granite as it is the magmatic pulse occurring close to the migmatization age, or possibly another unexposed contemporaneous pluton.

A Paleocene migmatization event has not been reported in Sonora, but a Laramide tectonic event is assumed by many authors to have synchronously occurred with the Laramide magmatic arc (Haxel *et al.*, 1984; Goodwin and Haxel, 1990). Tectonic structures recording the Laramide orogeny are more clearly dated from northwestern Sonora, where Iriondo *et al.* (2005) dated white micas developed in thrust faults affecting plutons of Late Cretaceous age. Similarly, in south-central Arizona, ductile thrusting started in Late Cretaceous time and culminated about 60 to 58 Ma ago (Haxel *et al.*, 1984). According to Haxel *et al.* (1984), latest Cretaceous to early Tertiary metamorphic rocks in that region share common features of an orogenic event characterized by thin-skinned faulting and thickening in the upper crust, while the

middle crust was traversed by deep-seated upthrust faults reaching amphibolite facies conditions with associated migmatization.

The El Gato diorite and the El Pajarito granite are part of the several nested plutons that compose the El Jaralito batholith and they have similar U-Pb ages to the El Babizo granite and the La Aurora granodiorite, which crop out further north within the batholith (González-León *et al.*, 2011). Similarly, the Puerta del Sol granodiorite, which occupies a large outcrop in the study area, extends to the north forming an important part of the El Jaralito batholith. The U-Pb zircon age of 49.1 ± 0.46 Ma obtained for the Puerta del Sol pluton is closely similar to U-Pb ages of 49.95 ± 1.05 and 51.26 ± 1.0 Ma reported by González-León *et al.* (2011) for this pluton to the north, in Sierra El Jaralito.

Considering that Laramide magmatism in central Sonora mostly ended at ~ 50 Ma (Gans, 1997; González-León *et al.*, 2011), the emplacement of the Puerta del Sol granodiorite occurred near the end of that event. El Oquimonis granite, emplaced at *ca.* 42 Ma, well-after crystallization of the Puerta del Sol pluton, might be part of the regionally scarce, transitional magmatism between the Laramide event and the volcanism of the Sierra Madre Occidental (Ferrari *et al.*, 2007). The only other dated rocks with ages near 40 Ma include an andesite and a rhyolite reported by Damon *et al.* (1983) (K-Ar ages) and a dacite dome dated by Gans (1997) at 43.8 ± 0.2 Ma ($^{40}\text{Ar}/^{39}\text{Ar}$). The latter author considered that the dacite dome was formed during a phase of minor exhumation, slow cooling and erosion that occurred at the end of the Laramide event and just before the onset of magmatism of the Sierra Madre Occidental event and metamorphic core complex formation (Wong *et al.*, 2010).

The Laramide plutons herein reported are mostly high-K calc-alkaline, metaluminous to slightly peraluminous (except for the peraluminous El Oquimonis granite) (Figure 4). The REE patterns

characterized by LREE enrichments suggest an important degree of crystal fractionation. The peraluminous leucogranites however have different REE patterns. The El Oquimonis granite is relatively depleted in LREE and has a pronounced negative Eu anomaly, which resembles the pattern shown by the *ca.* 57 Ma Huépac granite, a two-mica, garnet-bearing granite that crops out to the north within El Jaralito batholith (González-León *et al.*, 2011). Similarly, the samples of the garnet-bearing El Pajarito granite have a large negative Eu anomaly and a nearly flat REE pattern with clearly higher REE enrichments compared to the rest of the samples (Figure 5a). Peraluminous leucogranites are generally interpreted to be formed by partial melting of mature continental crust or to be derived from metasedimentary rocks (Pitcher, 1993). That may be the case for the El Pajarito and El Oquimonis granites since roof pendants of metasedimentary rocks are observed in several places within these plutons (Figure 2).

In the primitive mantle normalized multi-element diagrams of the Laramide granites, all of them show consistent patterns with negative anomalies of Nb-Ta, Sr, P and Ti that are also consistent with a continental magmatic arc origin, while the negative initial epsilon Nd values support important crustal assimilation by the mantle-derived magmas. The REE-pattern of these plutons are similar to the REE-patterns reported for other Laramide plutons of central Sonora (*e.g.* Valencia-Moreno *et al.*, 2001; Roldán-Quintana *et al.*, 2009; González León *et al.*, 2011), and their Sr, Nd and Pb isotope compositions are also within the range of values reported for Laramide plutons of central Sonora (summarized in González León *et al.*, 2011) (Figure 6).

Miocene syn-extensional plutonism

The current understanding on the initiation and evolution of the Sierra Mazatán core complex (Figure 1) was refined by structural, geochronological and thermochronological studies by Vega-Granillo and Calmus (2003) and Wong and Gans (2003, 2008). Wong and Gans (2008) considered the Puerta del Sol area as part of the lower plate of the Sierra Mazatán metamorphic core complex and concluded that the low-angle normal fault that unroofed the complex had two major tectonic slip events: the first from 25 to 23 Ma, and the second from 21 to 16 Ma. The mylonitization of the footwall rocks in the western part of the complex formed synchronously with the early fault slip, also the total amount of slip along the fault was estimated to be of 15 to 20 km, on the basis of $^{40}\text{Ar}/^{39}\text{Ar}$ thermochronology. Similarly, they inferred that the deepest exhumed and most tilted part of the footwall was its western portion, which originally resided at a depth of 10 – 30 km at 21 Ma, prior to exhumation.

For the study area, Wong and Gans (2008) reported three $^{40}\text{Ar}/^{39}\text{Ar}$ ages from the Puerta del Sol granodiorite (Figure 2). Biotites from their PS3 and PS2 samples yielded plateau ages of 24.4 ± 0.1 Ma and 22.0 ± 0.1 Ma, respectively, while K-feldspar from sample PS1 yielded a complex age spectrum that qualitative indicate rapid cooling from 21 to 17.5 Ma (Wong and Gans, 2008).

According to the U-Pb zircon age for the El Garambullo gabbro, it was emplaced at 19.83 ± 0.18 Ma, while $^{40}\text{Ar}/^{39}\text{Ar}$ dating indicates a cooling age for plagioclase of 17.4 ± 1.0 Ma (Figures 7u and 8b), which coincides with the second phase of tectonic denudation in the Mazatán metamorphic core complex (Wong and Gans, 2008). The El Garambullo gabbro was emplaced well after the phase of mylonitization, which did not affect it, although it contains mylonitized xenoliths of the Puerta del Sol granodiorite. The other K-Ar and $^{40}\text{Ar}/^{39}\text{Ar}$ cooling ages obtained for the El Palofierral, Puerta del Sol and El Oquimonis plutons range from ~26 and ~20 Ma and are within the range of ages reported for the Sierra Mazatán metamorphic core complex denudation (Vega-Granillo and Calmus, 2003; Wong and Gans, 2008). The K-Ar age of 19.2 ± 1.2 Ma obtained for the Las Mayitas granodiorite

however may be close to its age of emplacement, as that age is similar to the age of crystallization of the El Garambullo gabbro with which it shares mingling and other related structures.

Geochemically, the El Garambullo and Las Mayitas plutons display features fitting the *ca.* 25 to 16 Ma crustal “contaminated” orogenic volcanic rocks reported from Sonora (Gómez-Valencia *et al.*, 2015). They show relatively negative Nb-Ta anomalies and negative initial epsilon Nd values suggesting a continental magmatic arc origin and important crustal assimilation by the mantle-derived magmas. They however are clearly related to tectonic extension and are emplaced in the western sector of the Sierra Mazatán core complex, where the highest exhumation rates occurred (Wong and Gans, 2008). The coeval nature of these mafic and felsic plutons also suggest that they may be part of the magmatic systems that generated the Miocene bimodal volcanism that is interbedded with the clastic sediments of the Báucarit Formation, which was extruded along high-angle normal faults during the regional extensional event that exhumed the metamorphic core complex systems in Sonora. Three samples of mafic rocks dated by Wong and Gans (2008) from the adjacent basin-fill of the Sierra Mazatán metamorphic core complex have ages from *ca.* 18 to 15 Ma (samples MV-2, MV-3 and MV-4 in their figures 3 and 5), which constrain the younger time of denudation and sedimentation for this complex.

CONCLUSIONS

The Puerta del Sol area, located in central Sonora, Mexico, holds a record of Laramide arc to Miocene syn-extensional magmatism that is represented by plutons that range in age from *ca.* 71 to 20 Ma. The area is part of the El Jaralito batholith and is the northern prolongation of the Sierra Mazatán metamorphic core complex lower plate. The basement is represented by the El Palofierral orthogneiss whose *ca.* 1.7 Ga age and isotopic signature is characteristic of the Paleoproterozoic basement of the Caborca block. Metamorphosed carbonate rocks of this terrane occur as pendants on the Laramide plutons.

The Laramide plutons are the El Gato diorite, El Pajarito and El Oquimonis granites and the Puerta del Sol granodiorite. The oldest is El Gato diorite with an emplacement age of 71.29 ± 0.45 Ma and the youngest is the 41.78 ± 0.32 Ma El Oquimonis granite. The younger age of the El Oquimonis pluton however might indicate a relation to the regionally scarce, transitional magmatism occurring between the Laramide event and the magmatism of the Sierra Madre Occidental. A *ca.* 68 – 59 Ma migmatization event affecting the El Palofierral orthogneiss and the El Gato and El Pajarito plutons might be related to partial melting associated with deep-seated emplacement of the 67.9 ± 0.43 Ma El Pajarito granite. The age of the Laramide plutons in the Puerta del Sol area are within the age range reported for plutons of the El Jaralito batholith to the north, and the extensive outcrops of the Puerta del Sol granodiorite extend further to the north into the Sierra El Jaralito.

The El Garambullo gabbro and the Las Mayitas granodiorite are two small plutons that were emplaced at *ca.* 20 Ma in the western part of the metamorphic core complex footwall; mingling structures and textures are found at the contact between these Miocene plutons. An $^{40}\text{Ar}/^{39}\text{Ar}$ age of 17.4 ± 1.0 Ma, in plagioclase for the El Garambullo gabbro is interpreted as a cooling age for this pluton. U-Pb, $^{40}\text{Ar}/^{39}\text{Ar}$ and K-Ar ages for both plutons also suggest that they were emplaced synchronous with the second phase of tectonic denudation of the Sierra Mazatán metamorphic core complex, which took place from 21 to 16 Ma (Wong and Gans, 2008). Accordingly, these plutons are not affected by mylonitization that occurred during the first phase

of exhumation, from 25 to 23 Ma (Wong and Gans, 2008). K-Ar and $^{40}\text{Ar}/^{39}\text{Ar}$ dates of ~26 to 20 Ma obtained for the El Palofieral, Puerta del Sol and El Oquimonis plutons are cooling ages corresponding to the time of denudation reported for the Sierra Mazatán metamorphic core complex (Vega-Granillo and Calmus, 2003, Wong and Gans, 2008).

The Laramide plutons and the migmatized rocks of the study area have geochemical compositions that indicate magmas formed in a subduction-related continental arc, a setting previously suggested for that magmatism in Sonora (Valencia-Moreno *et al.*, 2001; Roldán-Quintana *et al.*, 2009; González León *et al.*, 2010; González León *et al.*, 2011; Gómez-Valencia *et al.*, 2015), while their Sr, Nd and Pb isotope compositions are within the range of values reported for Laramide plutons of central Sonora (summarized in González León *et al.*, 2011). Geochemical signatures of the Miocene plutons also show affinity with arc-derived, crustal contaminated magmas but their age and tectonic setting indicate they were formed during deep exhumation and regional extension. Geochemical and isotopic data to better characterize the Late Cretaceous and Cenozoic magmatism in Sonora are still scarce and further work is required for more comprehensive petrogenetic interpretations.

ACKNOWLEDGMENTS

The main author acknowledges and thanks the Consejo Nacional de Ciencia y Tecnología (CONACyT) for scholarship 376860 granted to support his graduate studies at the Departamento de Geología, Universidad de Sonora. Geochronologic and geochemical analysis for this work were supported by Project 24893 granted by CONACyT to one of the authors (González-León, C.M.). Victor Valencia of the LaserChron Center of the Department of Geosciences of the University of Arizona, Carlos Ortega-Obregón at Centro de Geociencias, UNAM, and Paty Girón, Instituto de Geología, UNAM are also acknowledged for analytical support. Our thanks are also expressed to Pablo Peñaflor Escárcega and Aimeé Orci, Estación Regional del Noroeste, Instituto de Geología, UNAM for their help in sample preparation and thin sections elaboration. Reviews by Dr. Martín A. Valencia Moreno and one of the Editors greatly improved this manuscript and are greatly appreciated.

SUPPLEMENTARY MATERIAL

Supplementary Tables S1 "U-Pb geochronology data. Laboratorio de Estudios Isotópicos, Centro de Geociencias, UNAM." and S2 "U-Pb geochronology data. LaserChron Center, University of Arizona." can be found at the journal web site <<http://rmcg.unam.mx/>>, in the table of contents of this issue.

REFERENCES

- Anderson, T.H., Silver, L.T., 2005, The Mojave-Sonora megashear —Field and analytical studies leading to the conception and evolution of the hypothesis: Geological Society of America, Special Paper 393, 1-50, doi: 10.1130/0-8137-2393-0.1.
- Anderson, T.H., Silver, L.T., Salas, G.A., 1980, Distribution and U-Pb of some lineated plutons, northwestern Mexico, in Crittenden Jr., M.D., Coney, P.J., Davis, G.H. (eds.), Cordilleran Metamorphic Core Complexes: Geological Society of America, Memoir 153, 269-286.
- Arvizu, H.E., Iriando, A., Izaguirre, A., Chávez-Cabello, G., Kamenov, G.D., Solís-Pichardo, G., Foster, D.A., Lozano-Santa Cruz, R., 2009, Rocas graníticas pérmicas en la Sierra Pinta, NW de Sonora, México: Magmatismo de subducción asociado al inicio del margen continental activo del SW de Norteamérica: Revista Mexicana de Ciencias Geológicas, 26(3), 709-728.
- Barra, F., Ruiz, J., Valencia, V. A., Ochoa-Landín, L., Chesley, J.T., Zurcher, L., 2005, Laramide porphyry Cu-Mo mineralization in northern México: Age constraints from Re-Os geochronology in molybdenites: Economic Geology, 100, 1605-1616. doi:10.2113/gsecongeo.100.8.1605.
- Bennet, V.C., DePaolo, D.J., 1987, Proterozoic crustal history of the western United States as determined by neodymium isotopic mapping: Geological Society of America Bulletin, 99, 674-685.
- Bronner, G., Radelli, L., 1996, Study of a NE-SW Eocene compressive phase in the Paleocene granites of the Aconchi Massif, central Sonora, Mexico: Boletín del Departamento de Geología de la Universidad de Sonora, 13, 1-9.
- Calles-Montijo, R., 1999, Evolución tectonosedimentaria de las cuencas terciarias: porción sur cuenca de Ures y Punta de Agua, Sonora central, México: Hermosillo, Sonora, México, Universidad de Sonora, Departamento de Geología, Tesis de Maestría, 67 pp.
- Calmus, T., Vega-Granillo, R., Lugo-Zazueta, R., 2011, Evolución geológica de Sonora durante el Cretácico Tardío y el Cenozoico, in Calmus, T. (ed.), Panorama de la Geología de Sonora, México: Universidad Nacional Autónoma de México, Instituto de Geología, Boletín, 118, 227-266.
- Clark, K.F., Foster, C.T., Damon, P.E., 1982, Cenozoic mineral deposits and subduction-related magmatic arcs in Mexico: Geological Society of America Bulletin, 93, 533-544.
- Coney, P.J., 1980, Cordilleran metamorphic core complexes: An overview, in Crittenden Jr., M.D., Coney, P.J., Davis, G.H. (eds.), Cordilleran Metamorphic Core Complexes, Geological Society of America, Memoir 153, 7-34.
- Coney, P.J., Reynolds, S.J., 1977, Cordilleran Benioff zones: Nature, 270, 403-406.
- Cuéllar-Cárdenas, M.A., Nieto-Samaniego, A.F., Levresse, G., Alaniz-Álvarez, S.A., Solari, L., Ortega-Obregón, C., López-Martínez, M., 2012, Límites temporales de la deformación por acortamiento Laramide en el centro de México: Revista Mexicana de Ciencias Geológicas, 29(1), 179-203.
- Damon, P.E., Mauger, R.L., 1966, Epeirogeny-orogeny viewed from the Basin and Range Province: Transactions Society of Mining Engineers, 235, 99-112.
- Damon, P.E., Shafiqullah, M., Roldán-Quintana, J., Cochemé, J.J., 1983, El Batolito Laramide (90-40 Ma) de Sonora, in Convención Nacional XV: Guadaluajara, Jal., México, Asociación de Ingenieros de Minas, Metalurgistas y Geólogos de México (AIMMGM), 63-95.
- De la Roche, H., Leterrier, J., Grandclaude, P., Marchal, M., 1980, A classification of volcanic and plutonic rocks using R1-R2 diagram and major element analyses -its relationships with current nomenclature: Chemical Geology, 29, 183-210.
- Del Río Salas, R., Ochoa-Landín, L., Ruiz, J., Eastoe, C., Meza-Figueroa, D., Zúñiga-Hernández, H., Mendiivil-Quijada, H., Quintanar-Ruiz, F., 2013, Geology, stable isotope, and U-Pb geochronology of the Mariquita porphyry copper and Lucy Cu-Mo deposits, Cananea District, México: A contribution to regional exploration: Journal of Geochemical Exploration 124, 140-154.
- Dickinson, W.R., Snyder, W.S., 1978, Plate tectonics of the Laramide orogeny, Matthews, V. III, Laramide folding associated with basement block faulting in the western United States: Geological Society Memoir, 151, 355-366.
- Farmer, G.L., Bowring, S.A., Matzel, J., Espinoza-Maldonado, G., Fedo, C., Wooden, J.L., 2005, Proterozoic Mojave province in northwestern Mexico? Isotope and U-Pb zircon geochronologic studies of Precambrian and Cambrian crystalline and sedimentary rocks, Caborca, Sonora configuration, in Anderson, T.H., Nourse, J.A., McKee, J., Steiner, M.B. (eds.), The Mojave-Sonora Megashear Hypothesis: development, assessment, and alternatives: Geological Society of America, Special Paper 393, 183-198.
- Ferrari, L., Valencia-Moreno, M., Bryan, S., 2007, Magmatism and tectonics of the Sierra Madre Occidental and its relation with the evolution of the western margin of North America, in Alaniz-Álvarez, S.A., Nieto-Samaniego, A.F. (eds.), Geology of México: Celebrating the Centenary of the Geological Society of México: Geological Society of America Special Paper 422, 1-39, doi: 10.1130/2007.2422(01).
- Gans, P.B., 1997, Large-magnitude Oligo-Miocene extension in southern Sonora: implications for the tectonic evolution of northwestern Mexico:

- Tectonics, 16, 388-408.
- Gehrels, G., Valencia, V., Pullen, A., 2006, Detrital Zircon Geochronology by Laser Ablation Multicollector ICPMS at the Arizona LaserChron Center, in Olszewski, T.D. (ed.), *Geochronology: Emerging Opportunities: Paleontology Society Papers*, 12, 67-76.
- Gómez-Valencia, A.M., Vidal-Solano, J.R., López-Martínez, M., Vega-Granillo, R., Pallares, C., 2015, Petrografía, geoquímica y geocronología del magmatismo orogénico en Rayón: Características petrológicas de los últimos magmas asociados a la subducción en Sonora, México: *Revista Mexicana de Ciencias Geológicas*, 32(2), 219-238.
- González-Becuar E., 2013, Aportación a la tectónica laramídica de Sonora central: geología, geocronología y geoquímica de la Sierra El Pajarito: Universidad de Sonora, Departamento de Geología, Tesis de maestría, 126 pp.
- González-León, C.M., Valencia, V., López, M., Bellon, H., Valencia Moreno, M.A., Calmus, T., 2010, The Arizpe sub-basin: sedimentary and magmatic evolution of the Basin and Range in north-central Sonora, México: *Revista Mexicana de Ciencias Geológicas*, 27(2), 292-312.
- González-León, C.M., Solari, L., Solé, J., Duca, M.N., Lawton, T.F., Bernal, J.P., González Becuar, E., Gray, F., López Martínez, M., Lozano Santacruz, R., 2011, Stratigraphy, geochronology, and geochemistry of the Laramide magmatic arc in north-central Sonora, Mexico: *Geosphere*, 7, 1392-1418.
- González-León, C.M., Solari, L., Valencia-Moreno, M., Rascón Heimpel, M.A., Solé, J., González Becuar, E., Lozano Santacruz, R., Pérez Arvizu, O., 2017, Late Cretaceous to early Eocene magmatic evolution of the Laramide arc in the Nacozari quadrangle, northeastern Sonora, Mexico and its regional implications: *Ore Geology Reviews*, 81, 1137-1157, <http://dx.doi.org/10.1016/j.oregeorev.2016.07.020>.
- Goodwin, L., Haxel, G., 1990, Structural evolution of the southern Baboquivari Mountains, Arizona: *Tectonics*, 9, 1077-1095.
- Haxel, G.H., Tosdal, R.M., May, D.J., Wright, J.E., 1984, Latest Cretaceous and early Tertiary orogenesis in south-central Arizona: thrust faulting, regional metamorphism and granitic plutonism: *Geological Society of America Bulletin*, 95, 631-653.
- Housh, T.B., McDowell, F.W., 2005, Isotope provinces in Laramide and mid-Tertiary igneous rocks of northwestern Mexico (Chihuahua and Sonora) and their relation to basement configuration, in Anderson, T.H., Nourse, J.A., McKee, J.W., Steiner, M.B. (eds.), *The Mojave-Sonora megashear hypothesis: Development, assessment, and alternatives: Geological Society of America Special Paper*, 393, 671-692, doi: 10.1130/2005.2393(25).
- Iriondo, A., Premo, W.R., 2011, Las rocas cristalinas proterozoicas de Sonora y su importancia para la reconstrucción del margen continental SW de Laurentia—La pieza mexicana del rompecabezas de Rodinia, in Calmus, T. (ed.), *Panorama de la geología de Sonora, México: Universidad Nacional Autónoma de México, Instituto de Geología, Boletín* 118, 25-55.
- Iriondo, A., Premo, W.R., Martínez-Torres, L.M., Budahn, J.R., Atkinson, W.W., Jr., Siems, D.F., Guarás-González, B., 2004, Isotopic, geochemical, and temporal characterization of Proterozoic basement rocks in the Quitovac region, northwestern Sonora, Mexico: Implications of the reconstruction of the Southwestern margin of Laurentia: *Geological Society of America Bulletin*, 116, 154-170.
- Iriondo, A., Martínez-Torres, L.M., Kunk, M.J., Atkinson, W.W., Jr., Premo, W.R., McIntosh, W.C., 2005, Northward Laramide thrusting in the Quitovac region, north-western Sonora, Mexico: Implications for the juxtaposition of Paleoproterozoic base-ment blocks and the Mojave-Sonora megashear hypothesis, in Anderson, T.H., Nourse, J.A., McKee, J.W., Steiner, M.B. (eds.), *The Mojave-Sonora Megashear Hypothesis: Development, assessment, and alternatives: Geological Society of America, Special Paper* 393, 631-669.
- Irvine, T.N., Baragar, W.R.A., 1971, A guide to the chemical classification of the common volcanic rocks: *Canadian Journal of Earth Sciences*, 8, 523-548.
- Kuno, H., 1968, Differentiation of basalt magmas, in Hess, H.H., Poldervaart, A.A. (eds.), *Basalts: The Poldervaart Treatise on Rocks of Basaltic Composition*, 2: New York, Interscience, 623-688.
- Le Bas, M.J., Le Maitre, R.W., Streckeisen, A., Zanettin, B., 1986, A chemical classification of volcanic rocks based on the Total Alkali-Silica diagram: *Journal of Petrology*, 27, 745-750.
- Lozano-Santa Cruz, R., Bernal J.P., 2005, Characterization of a new set of eight geochemical reference materials for XRF major and trace element analysis: *Revista Mexicana de Ciencias Geológicas*, 22(3), 329-344.
- McDonough, W.F., Sun, S.S., 1995, The Composition of the Earth: *Chemical Geology*, 120, 223-253.
- McDowell, F.W., Roldán-Quintana, J., Connelly, J.N., 2001, Duration of Late Cretaceous-early Tertiary magmatism in east-central Sonora, Mexico: *Geological Society of America Bulletin*, 113, 521-531.
- Mori, L., Gómez-Tuena, A., Cai, Y., Goldstein, S.L., 2007, Effects of prolonged flat subduction on the Miocene magmatic record of the central Trans-Mexican Volcanic Belt: *Chemical Geology*, 244, 452-473.
- Nourse, J.A., Anderson, T.H., Silver, L.T., 1994, Tertiary metamorphic core complexes in Sonora, northwestern Mexico: *Tectonics*, 13, 1161-1182.
- Nourse, J.A., Premo, W.R., Iriondo, A., Stahl, E.R., 2005, Contrasting Proterozoic basement complexes near the truncated margin of Laurentia, northwestern Sonora-Arizona international border region in Anderson, T.H., Nourse, J.A., McKee, J.W., Steiner, M.B., (eds.), *The Mojave-Sonora megashear hypothesis: Development, assessment, and alternatives: Geological Society of America Special Paper*, 393, 123-182.
- Pearce, J.A., Harris, N.B.W., Tindle, A.G., 1984, Trace element discrimination diagrams for the tectonic interpretation of granitic rocks: *Journal of Petrology*, 25, 956-983.
- Peccerillo, A., Taylor, S.R., 1976, Geochemistry of Eocene calc-alkaline volcanic rocks from the Kastamonu area, Northern Turkey: *Contributions to Mineralogy and Petrology*, 58, 63-81.
- Pérez-Segura, E., González-Partida, E., Valencia, V.A., 2009, Late Cretaceous adakitic magmatism in east-central Sonora, México, and its relation to Cu-Zn-Ni-Co skarns: *Revista Mexicana de Ciencias Geológicas*, 26(2), 411-426.
- Pérez-Segura, E., González-Partida, E., Roldán-Quintana, J., 2013, Genetic implications of new Sr and Nd isotopic data of the intrusive rocks from the Laramide arc in northern Sonora, Mexico: *Journal of Iberian Geology*, 39, 131-146.
- Pitcher, W.S., 1993, *The nature and origin of granite*: London, Chapman & Hill, 321 pp.
- Radelli, L., 1986, An essay on the southern Basin and Range: *Boletín del Departamento de Geología de la Universidad de Sonora*, 3, 51-146.
- Radelli, L., Lucero-Bernal, V., Macías-Valdez, G., 1995, The Huepac continental volcanic arc of central Sonora, México: Eocene compressional deformation, magma underplating, crustal melting, and magmatism: *Boletín del Departamento de Geología de la Universidad de Sonora*, 12, 109-204.
- Roldán-Quintana, J., 1989, Geología de la Hoja Baviácora, Sonora: Universidad Nacional Autónoma de México, Instituto de Geología, *Revista*, 8, 1-14.
- Roldán-Quintana, J., 1991, Geology and chemical composition of the Jaralito and Aconchi batholiths in east-central, Sonora, Mexico, in Pérez-Segura, E., Jacques-Ayala, C. (eds.), *Studies in Sonoran Geology: Geological Society of America, Special Paper*, 254, 69-80.
- Roldán-Quintana, J., McDowell, F.W., Delgado-Granados, H., Valencia-Moreno, M., 2009, East-west variations in age, chemical and isotopic composition of the Laramide batholith in southern Sonora, Mexico: *Revista Mexicana de Ciencias Geológicas*, 26(3), 543-563.
- Sawyer, E.W., 2008, *Atlas of Migmatites: The Canadian Mineralogist, Special Publication* 9, 371 pp.
- Shand, S.J., 1943, *Eruptive rocks: Their genesis, composition, classification, and their relation to ore-deposits with a chapter on meteorites*: New York, John Wiley & Sons, 444 pp.
- Solari, L.A., Gómez-Tuena, A., Bernal, J.P., Pérez-Arvizu, O., Tanner, M., 2010, U-Pb zircon geochronology by an integrated LA-ICPMS microanalytical workstation: achievements in precision and accuracy: *Geostandards and Geoanalytical Research*, 34, 5-18.
- Solari, L.A., Ortega-Obregón, C., Bernal, J.P., 2015, U-Pb zircon geochronology by LAICPMS combined with thermal annealing: Achievements in precision and accuracy on dating standard and unknown samples: *Chemical Geology*, 414, 109-123.
- Sun, S.S., McDonough, W.F., 1989, Chemical and isotopic systematics of oceanic basalts: implications for mantle composition and processes, in Saunders, A.D., Norry, M.J., (eds.) *Magmatism in Ocean Basins: Geological Society of London Special Publication* 42, 313-345.
- Valencia, V.A., Ruiz, J., Barra, F., Gehrels, G.E., Duca, M.N., Titley, S., Ochoa-Landín, L., 2005, U-Pb zircon and Re-Os molybdenite geochronology from La Caridad porphyry copper deposit: Insights from the duration of

- magmatism and mineralization in the Nacozari district, Sonora, Mexico: *Mineralium Deposita*, 40, 175-191.
- Valencia-Moreno, M., Ruiz, J., Barton, M., Patchett, P.J., Zurcher, L., Hodkinson, D.G., Roldán-Quintana, J., 2001, A chemical and isotopic study of the Laramide granitic belt of northwestern Mexico: Identification of the southern edge of the North American Precambrian basement: *Geological Society of America Bulletin*, 113, 1409-1422.
- Valencia-Moreno, M., Ruiz, J., Ochoa-Landin, L.H., Martinez-Serrano, R., Vargas-Navarro, P., 2003, Geochemistry of the Coastal Sonora batholith, Northwestern Mexico: *Canadian Journal of Earth Sciences*, 40, 819-831.
- Vega-Granillo, R., Calmus, T., 2003, Mazatán metamorphic core complex, Mexico: Structures along the detachment fault and its exhumation evolution: *Journal of South American Earth Sciences*, 16, 193-204.
- Wilson, F.I., Rocha, S.V., 1949, Coal deposits of the Santa Clara district near Tónichi, Sonora, Mexico: U.S. Geological Survey Bulletin 962A, 80 pp.
- Wooden, J.L., DeWitt, E., 1991, Pb isotopic evidence for the boundary between the Early Proterozoic Mojave and central Arizona crustal provinces in western Arizona, in Karlstrom, K.E. (ed.), *Early Proterozoic Geology and Ore Deposits of Arizona*: Arizona Geological Society Digest, 19, 27-50.
- Wooden, J.L., Stacey, J.S., Howard, K.A., Doe, B.R., Miller, D.M., 1988, Pb isotopic evidence for the formation of Proterozoic crust in the southwestern United States, in Ernst, W.G. (ed.), *Metamorphism and Crustal Evolution, Western Conterminous United States*: Englewood Cliffs, New Jersey, Prentice-Hall, 68-86.
- Wong, M.S., Gans, P.B., 2003, Tectonic implications of early Miocene extensional unroofing of the Sierra Mazatan metamorphic core complex, Sonora, Mexico: *Geology*, 31, 953-956.
- Wong, M.S., Gans, P.B., 2008, Geologic, structural, and thermochronologic constraints on the tectonic evolution of the Sierra Mazatán core complex, Sonora, Mexico: New insights into metamorphic core complex formation: *Tectonics*, 27, TC4013, doi:10.1029/2007TC002173.
- Wong, M. S., Gans, P.B., Scheier, J., 2010, The ⁴⁰Ar/³⁹Ar thermochronology of core complexes and other basement rocks in Sonora, Mexico: Implications for Cenozoic tectonic evolution of northwestern Mexico: *Journal of Geophysical Research*, 115, B07414, doi: 10.1029/2009JB007032.

Manuscript received: august 17, 2016

Corrected manuscript received: february 14, 2017

Manuscript accepted: february 15, 2017